2010

Small Molecule Caspase Inhibitors Using Isatin and Oxindole Scaffolds and a Combinatorial Approach

Hagar Mahmoud Abdallah
Wright State University

SMALL MOLECULE CASPASE INHIBITORS USING ISATIN AND OXINDOLE SCAFFOLDS AND A COMBINATORIAL APPROACH

A thesis submitted in partial fulfillment
of the requirements for the degree of
Master of Science

By

HAGAR MAHMOUD ABDALLAH
B.S., Wright State University, 2008

2010
Wright State University

WRIGHT STATE UNIVERSITY

SCHOOL OF GRADUATE STUDIES

December 1, 2010

I HEREBY RECOMMEND THAT THE THESIS PREPARED UNDER MY SUPERVISION BY Hagar Mahmoud Abdallah ENTITLED Small Molecule Caspase Inhibitors Using Isatin and Oxindole Scaffolds and a Combinatorial Approach BE ACCEPTED IN PARTIAL FULFILLMENT OF THE REQUIREMENTS FOR THE DEGREE OF Master of Science.

Daniel Ketcha, Ph.D.
Thesis Director

Kenneth Turnbull, Ph.D.
Chair, Department of Chemistry
College of Science and Mathematics

Committee on
Final Examination:

Daniel Ketcha, Ph.D.

Kenneth Turnbull, Ph.D.

Eric Fossum, Ph.D.

Andrew T. Hsu, Ph.D.
Dean, School of Graduate Studies

ABSTRACT

Abdallah, Hagar, M. M.S., Department of Chemistry, Wright State University, 2010. Small Molecule Caspase Inhibitors Using Isatin and Oxindole Scaffolds and a Combinatorial Approach.

Quinolyl-valyl-O-methylaspartyl-[2,6-difluorophenoxy]-methyl ketone (Q-VD-OPh) is a next generation broad spectrum caspase inhibitor, the effectiveness and reduced toxicity of which can be partially attributable to the carboxyterminal O-phenoxy group as well as the amino terminal quinolyl groups. We seek to incorporate some of these unique recognition elements onto small molecule derived protease inhibitors with drug like properties. Specifically, heterocyclic scaffolds such as isatins and oxindoles. Thus, isatins bearing electron withdrawing groups on C-5 and 2,6-difluorobenzyl moieties have been prepared by analogy to the well studied N-substituted 5-pyrrololidinylsulfonyl isatins. Moreover, 3-benzylidene oxindole derivatives bearing these structural motifs have also been prepared and their effectiveness as apoptosis inhibitors was examined employing human Jurkat T cells.

TABLE OF CONTENTS

Page

I. INTRODUCTION AND GOALS 1

Apoptotic Cell Death 1

Goals. 2

II. BACKGROUND 3

Caspase Family of Cysteine Proteases 3

Peptide Inhibitors 5

Q-VD-OPh as a Broad Spectrum Caspase Inhibitor. 6

Small Molecule Inhibitors: 5-Nitroisatins.. 8

Structure Activity Relation (SAR) Studies. 9

Introduction of Oxindoles. 15

III. OBJECTIVES. 18

Proposed Project 18

Planned Reactions. 19

IV. RESULTS AND DISCUSSION

Reactions with Isatin. 24

Reactions with Oxindole. 28

E or *Z* Configuration Determination. 30

Compound **30** *E* or *Z* Determination. 35

Oxindole ^{13}C NMR Determination. 37

Compound **33** ^{13}C NMR Determination. 38

Active Compound **X** Determination. 40

Cathepsin and Calpain Testing. 44

Synthesis of the Inactive Compound **43**. 46

Compound **43** ^{13}C NMR Determination. 47

Nitroquinolines to Oxindoles 49

Active Compounds **32** and **31**. 51

Future Work 56

V. EXPERIMENTAL 57

VI. REFERENCES. 76

LIST OF FIGURES

Page

1. Poly (ADP-ribose)polymerase, a DNA Repair Enzyme. 3
2. Mesencephalons of Mice With and Without Q-VD-OPh Treatment 6
3. 5-Substituted Isatins and their Inhibition Constants. 10
4. Isatin Sulfonamides and their Inhibition Constants 11
5. 5-Pyrrolidinyl Isatin Sulfonamides and its Analogues. 13
6. Summary of the SAR Study Performed by WashU 14
7. Isatin Michael Acceptor by WashU 14
8. Model Conformation of Inhibitor **11** in Caspase-1. 17
9. Structural Summary of Previous and Proposed Small Molecule Inhibitors. 18
10. Structural Differences between *E* and *Z* Isomers 31
11. Biological Screen for Compound **28**. 32
12. Biological Screen for Compound **33**. 36
13. ^{13}C NMR Spectrum of Oxindole. 37
14. ^{13}C NMR Spectrum of Compound **33**. 39
15. Biological Screen for Impure Compound **X**. 42
16. Biological Screen of a Purer Form of Compound **X**. 43
17. Biological Screen of Pure Compound **X**. 44
18. ChemDraw ^{13}C NMR Shift Predictions for Compound **33** 46
19. ^{13}C NMR Spectrum of Compound **43** 48

20. Biological Screen for Compound **43**. 49

21. Biological Screen for Compound **32**. 52

22. ^{13}C NMR Spectrum of Compound **32**. 53

23. Biological Screen for Compound **31**. 55

LIST OF TABLES

Page

1. Comparison of Phenoxymethyl and Pyridinoxymethyl Rings. 13

2. N-alkylations on Isatin using KF/Alumina and CaH_2 Base 25

3. Aldol Condensations using 5-Nitroindolin-2-one and Aldehydes 29

4. Aldol Condensations using Indolin-2-one and Aldehydes. 34

ACKNOWLEDGEMENTS

I would like to begin by thanking my family and friends for all of their love and support throughout my years here at WSU. They have been by my side in every decision that I have made and have supported me the entire time. Without their help and support, I would not be where I am today.

I would like to thank Dr. Daniel Ketcha for teaching me everything I know about organic synthesis. When I began in his lab two years ago, I knew very little about proper technique in the lab and about different equipment. He helped me learn it all and was actually with me in the lab teaching me the different techniques and the logistics of organic synthesis. I am deeply grateful to him not only for his help in the lab, but for his support with everything outside of the lab as well. He has helped me with my classes and answered any questions that I may have had, even the ones that may seem to be a "stupid" question. He has always been supportive throughout my time in his lab and I thank him very much for all he has done for me.

I would also like to thank my committee members Dr. Ken Turnbull and Dr. Eric Fossum for their support as well. I have also asked them many questions throughout my time here and they have always been there to answer them. Thank you both for your support and kindness.

I would also like to thank Dr. Thomas L. Brown and Apoptrol LLC. for their contributions to this research. Dr. Brown has been very patient with the biological testing and the screening of all of the compounds that we have sent to him. I am deeply grateful to him and greatly appreciate all of the hard work and effort put forth by him and his team.

Last but not least, I want to thank the rest of the Chemistry department's faculty, students and staff for a great graduate school experience. I will always remember the great times we had on campus, in the labs and in the classroom.

INTRODUCTION

Apoptosis, or programmed cell death, is a biological process in which individual old or damaged eukaryotic cells are signaled to commit suicide. It is a critical process in the maintenance of homeostasis between cell growth and cell death. As with most biological processes, excessive activity or inactivity can have many outcomes. Uncontrolled apoptosis has been associated with diseases such as cancer, Huntington's disease, and myocardial infarctions. Unlike necrosis, apoptosis is a clean, self contained process.[1] During necrotic cell death, the cell swells and eventually bursts. Cellular debris is left behind and can trigger an immune response; mainly inflammation.[1] During apoptosis, the cell will shrink upon itself and the DNA will fragment. The cell membrane will also collapse and the cell will split into small apoptotic bodies. These apoptotic bodies can then be phagocytosed by macrophages, a type of white blood cell.

During apoptosis, cell death can occur through two different signaling pathways: intrinsically and extrinsically. In the intrinsic pathway, the signal that triggers cell death comes from within the cell itself.[2] This can result from DNA damage, heat shock, or a defective cell cycle. This pathway involves the release of pro-apoptotic proteins from the mitochondria. In the extrinsic pathway, the death signal comes from outside of the cell through pro-apoptotic receptors on the cell membrane. Pro-apoptotic ligands bind to the pro-apoptotic receptors on the cell membrane. Once cell death is signaled, whether it is by an intrinsic or extrinsic signaling mechanism, a series of cysteinyl aspartic proteases

(caspases) are activated to carry out apoptosis. The purpose of this research is twofold: 1) to synthesize and characterize new, potent caspase inhibitors for biological screening and 2) to build a combinatorial library using isatin and oxindole scaffolds that may also have some biological activity. This work is based on previous research as well as new insight for possible inhibitor potency and combinatorial library synthesis.

BACKGROUND

Recent studies have shown that caspases are critical enzymes in the activation and execution of apoptosis. They have also been shown to play important roles in inflammation and cytokine maturation. Within the caspase family are caspases 2, 8, 9 and 10, which are the initiator caspases. These initiator caspases are signaled by intrinsic or extrinsic pathways of the apoptotic process and activate the effector caspases, which are caspases 3, 6 and 7. Caspases 1, 4 and 5 are reported to be involved in inflammation, not in apoptosis. Caspase-3 is the dominant effector caspase involved in the cleavage of DNA repair enzymes, nuclear lamins and regulatory proteins during apoptosis.[1, 2]

Caspases recognize a specific tetrapeptide chain within the amino acid sequence of the substrate (target), and that is the P_4-P_3-P_2-P_1 sequence.[3] These are the peptides that the caspase will cleave to begin apoptosis. It is very critical that the P_1 residue in the amino acid sequence be aspartic acid. For example, poly (ADP-ribose)polymerase or PARP, is a DNA repair enzyme that contains the cleavage sequence D-E-V-D (P_4-P_3-P_2-P_1) where D is aspartic acid, E is glutamic acid and V is valine as shown in **Figure 1**.

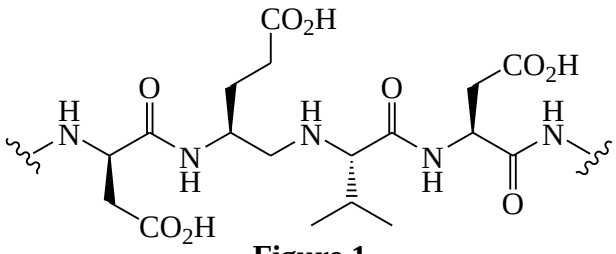

Figure 1

Caspases are a class of protease enzymes which catalyze the hydrolysis of amide bonds through nucleophilic attack by the activated cysteine thiol from the enzyme onto the amide carbonyl bond of the amino acid. The site of cleavage by the caspase (¯S-

Enzyme) is between the P_1 residue and the adjacent (carboxyterminal side) P_1' residue. The mechanism of this nucleophilic attack is shown in **Scheme 1.**

Scheme 1

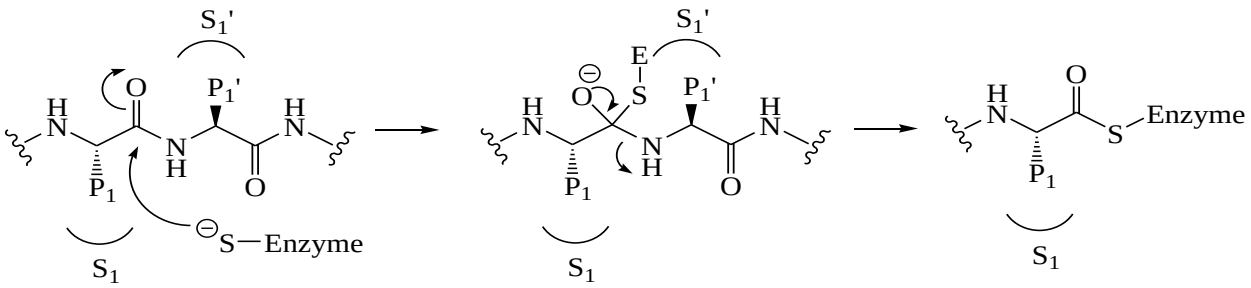

The corresponding binding sites for the P_4-P_3-P_2-P_1 residues on the substrates are called the S_4-S_3-S_2-S_1 subsites on the caspase respectively.[4] The cysteine residue of the caspase will attack the protein as a nucleophile at the amide carbonyl leading to the formation of a tetrahedral intermediate which upon reformation of the double bond will result in the subsequent cleavage of the peptide bond.

Peptide derived inhibitors which utilize this mechanism of action were the first type of caspase inhibitors studied in this field. In general, such inhibitors contain an electrophilic functionality termed the "warhead" which can in some cases react with the active-site cysteine residue. The warhead functionality is also very important for the ability to bind to the caspase. There are two types of warheads, the reversible and the irreversible functionalities. Reversible warheads are functional groups that bind to the caspase temporarily as through a tetrahedral intermediate and can then be released; these groups include ketones, aldehydes and nitriles. Irreversible warhead functional groups are usually good leaving groups, so when the caspase attacks as a nucleophile, the enzyme becomes covalently attached to the inhibitor and releasing (ideally) a non-toxic

and virtually harmless leaving group. Examples of irreversible warhead functional groups are acyloxymethylketones and halomethylketones.

Several peptide inhibitors have been synthesized and studied, including two potent inhibitors acetyl-aspartyl-glutamyl-N-(2-carboxy-1-formylethyl)-valinamide (Ac-DEVD-CHO)[5] and quinolyl-valyl-O-methylaspartyl-[2,6-difluorophenoxy]-methyl ketone (Q-VD-OPh)[5]. Ac-DEVD-CHO (**2**) is an effective and widely studied caspase inhibitor *in vitro*.

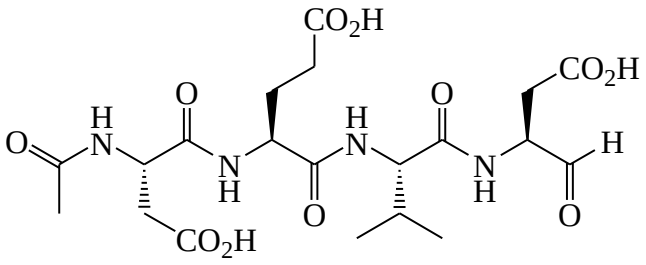

2

Unfortunately, compound **2** has a number of undesirable characteristics, including three CO_2H groups which decrease its ability to penetrate cells for *in vivo* studies. Also, the warhead functionality in this case is an aldehyde, which makes the inhibitor reversible. Aldehydes are also susceptible to attack by several classes of cellular nucleophiles in the body thereby limiting specificity; additionally, this group can also undergo oxidation.[4,5] Q-VD-OPh (**3**), a closely related peptide inhibitor was examined and found to have inhibition concentrations as low as 5μM.[5]

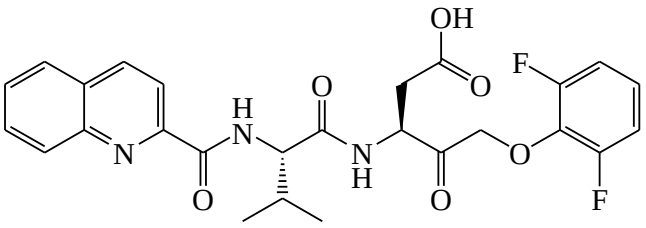

3

Q-VD-OPh was found to be non-toxic to cells, even at very high concentrations and contained an irreversible warhead functionality, the difluorophenoxy group. It was determined that the specificity and effectiveness of Q-VD-OPh was partially due to the difluorophenoxy warhead group.[5]

The broad spectrum caspase inhibitor Q-VD-OPh has been used to treat hypoxic-ischemic (HI) injury in the developing brain of P7 rats by Renolleau *et al.*[6] HI injury is directly linked to the development of apoptosis in a post-stroke brain. In this study, Q-VD-OPh was administered to rats of both genders after the onset of HI injury and the effects of the drug were monitored for a period of three weeks after administration. It was found that Q-VD-OPh greatly inhibited caspase-3 cleavage into its active p17 form, which is the conformation of the enzyme required to initiate apoptosis. Also, these authors found that the rats that were treated with Q-VD-OPh had significant neurological recovery in the first 48 h of recovery time. Another interesting find was that there was a significant difference in recovery and neuroprotection between the male and female rats. The females were more strongly protected neurologically than the males. Moreover, the females showed a decrease in the release of cytochrome c, a protein responsible for apoptosis. This study indicates that Q-VD-OPh was an effective caspase inhibitor in the central nervous system.

Q-VD-OPh has also been found to be an effective caspase inhibitor in Parkinson's disease (PD) and Huntington's disease (HD) models. A study conducted by Yang *et al.*[7] used a number of different mitochondrial toxins to model these two diseases. 1-Methyl-4-phenyl-1,2,3,6-tetrahydropyridine (MPTP) was used to model PD and 3-nitropropionic acid (3NP) and malonic acid (MA) were used to model HD.[7] These neurotoxins create lesions in the brain that model the affects of these neurodegenerative diseases. Using mice as the test subjects, Q-VD-OPh was injected 12 h before the injection of the neurotoxins and continued for several days. After 7 days, the mice were sacrificed and their brains were collected for examination. In **Figure 2**, a difference in the levels of neurotoxins can be clearly seen in the mesencephalons of the control mice and the mice treated with Q-VD-OPh.

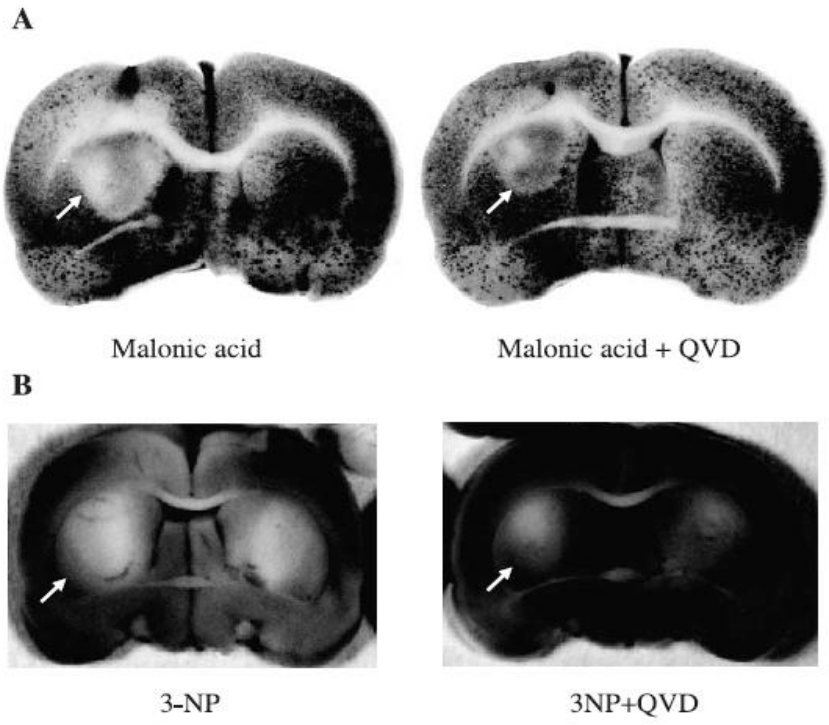

Figure 2

The arrows in **Figure 2** show the lesions formed from the neurotoxins in the mesencephalon.[7] The control mice show large lesions while the mice injected with Q-VD-OPh and the neurotoxins show smaller lesions. It is clear from **Figure 2** that Q-VD-OPh had a significant effect in protecting the mice against neurodegeneration.

While both Ac-DEVD-CHO and Q-VD-OPh are effective caspase inhibitors, they are not "drug-like" due to their peptide features. There are several disadvantages to peptide based inhibitors, including the fact that they are inherently peptides and can be metabolized *in vivo*; causing the drug to lack bioavailability. Also, they are relatively large and polar molecules, making it difficult to cross the Blood Brain Barrier (BBB). It is crucial for these inhibitors to cross the BBB for application to neurological disorders such as Parkinson's disease, Alzheimer's and Huntington's disease. Peptide inhibitors also have rapid physiological clearing times, by which they pass through the kidney and do not come back out again.

Consideration of the limitations inherent in the use of peptide-based caspase inhibitors for controlling cell death led to a search for potent small molecule inhibitors. High throughput screening of the SmithKline Beecham (SKB) compound collection for inhibitors of caspase-3 resulted in identification of 5-nitroisatins **4** and **5** which possessed IC_{50}s of 0.25 and 1 μM, respectively. The closely related unalkylated analogue **6** was only slightly less active (IC_{50} = 3 μM).[8] A correlation between the electron-withdrawing ability of the C-5 carbon and the potency of inhibition suggested that the electrophilicity of the C-3 carbonyl was critical for activity and that the mechanism of action involved addition of the catalytic cysteine residue of the enzyme to this functionality.

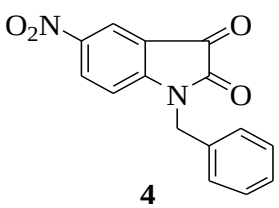

4

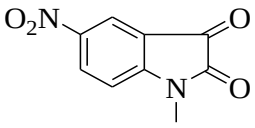

5

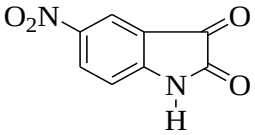

6

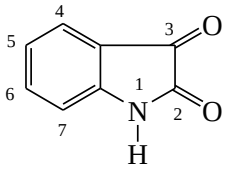

7

Isatin (**7**) is an attractive scaffold for many reasons; it is small and does not have any peptide-like features. Also, isatin-based drugs can potentially cross the BBB due to their relatively small size. Additionally, this scaffold allows for facile functionalization of both the aromatic ring as well as the heterocyclic nitrogen. Alkylation of the heterocyclic nitrogen can be performed under normal basic conditions whereas the introduction of electron withdrawing groups (EWGs) at the C-5 position on the aromatic ring can easily be accomplished by electrophilic aromatic substitution processes. Thus, this compound became the lead in a drug discovery program designed to develop potent, non-peptide caspase inhibitors. With two points of variability on the SKB lead being at the C-3 and the C-5 positions, a combinatorial library was produced using several EWGs at the C-5 position as well as various alkylating agents for the amide nitrogen.

GlaxoSmithKline (GSK) employed the lead compound found by SKB as a potential scaffold for a Structure -Activity Relationship (SAR) study designed to find the optimal combination of functional groups on the scaffold.[9] The first region inspected was the C-5 region. The main goal was to find an EWG that was irreducible *in vivo* and could withdraw electron density away from the C-3 region to allow for nucleophillic attack by

the activated cysteine residue of the caspase. While the lead compound contained a -NO_2 group as the EWG, unfortunately this group can be reduced in the body to amines and poses toxicity issues. Several different EWG on the C-5 position were synthesized and tested for inhibition capabilities as shown in **Figure 3**. The inhibition concentrations after 50% inhibition (IC_{50}) values are reported under each compound. It is important to note that the lower the IC_{50} the more potent the compound. The N-methyl isatin compound had a fairly high IC_{50} value, while just adding a -NO_2 group greatly increases its potency to 1μM.[9] Positioning a cyano group at the C-5 position led to an increase in potency to 0.6 μM, whereas an iodo substituent was found to decrease activity, presumably due to size. Finally, carboxylic acid derivatives were examined wherein the carboxylate ester was less effective for inhibition while the carboxylate salt practically ineffective.

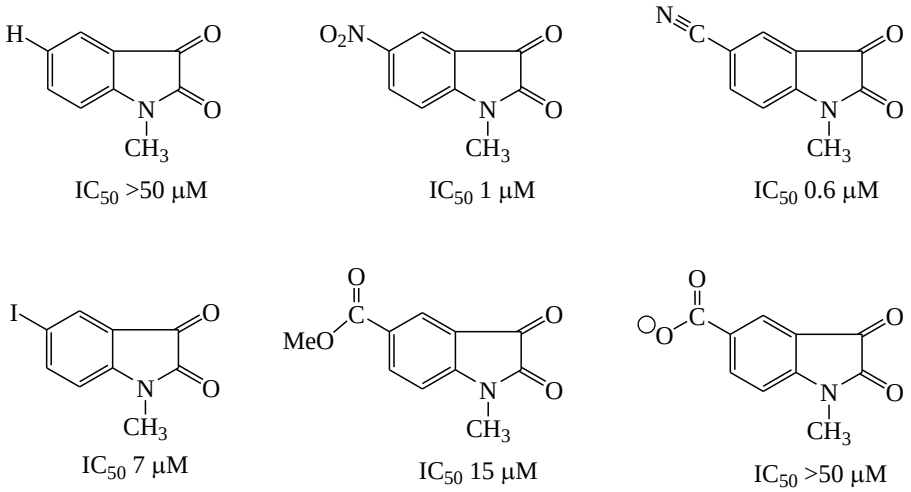

Figure 3

Further development led to the identification of the 5-N,N-dialkylisatin sulfonamide **8** as a potential inhibitor scaffold. This functionality was seemingly ideal

since it incorporated an irreducible, strongly EWG at the C-5 position, while allowing for further elaboration of the groups on the sulfonamide nitrogen so as to extend to the crucial S_2-S_4 subsites responsible for determining specificity between the different caspases.

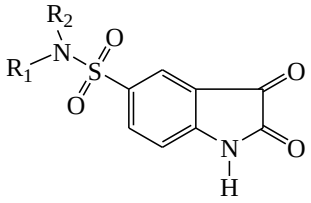

8

A group from Washington University in St. Louis (WashU) decided to build upon the GSK-SAR study.[10] They found that not only did the sulfonamide allow for various dialkylated species, it also allowed for the incorporation of rings of different sizes. Variation of the ring size on the sulfonamide was found to make a dramatic impact on the IC_{50} values with the results shown in **Figure 4**.

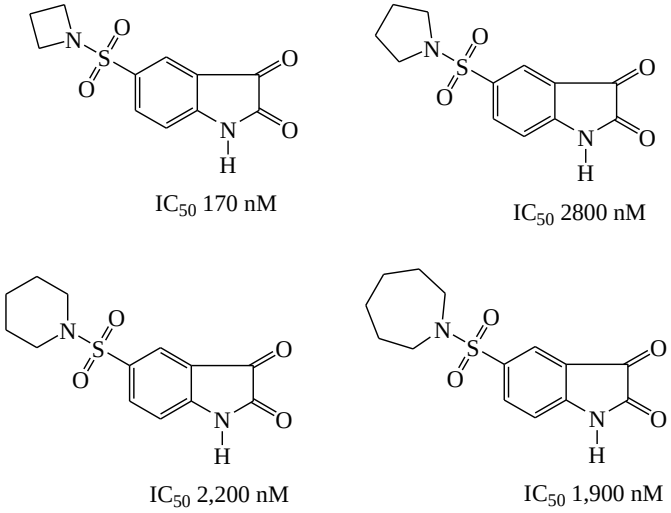

Figure 4

In general, based on the IC_{50}'s of the compounds in **Figure 4**, the larger the ring, the less potent the compound becomes. Even though the azetidine ring had a lower IC_{50},

the pyrrolidine ring was chosen as the optimal ring size for further studies due to the ease of adding groups to the pyrrolidine ring via chiral proline derivatives.[10] Ultimately, the WashU group found that addition of a 2-phenoxymethyl group in the (*S*)-configuration on the pyrrolidine ring resulted in an increase in potency of the resultant isatin sulfonamide to an IC_{50} of 240 nM. As stated earlier, elaboration of the substituents at the C-2 position of the pyrrolidine derivatives allows for extension into the S_2-S_4 pockets enabling modulation of both potency and specificity. For example, addition of a pyridinoxymethyl group in place of the phenoxymethyl group was also examined and the resultant compound was found more potent than the phenoxymethyl analogues.[10]

The next region of interest on the C-5 isatin sulfonamides was the isatin amide nitrogen. Alkylation of the amide nitrogen was found to greatly increase the potency of the inhibitor, as shown in **Figure 5.** Adding progressively larger groups on the amide nitrogen, such as a methyl group and a benzyl group, the inhibitor becomes progressively more potent. Groups such as benzyl and substituted benzyl groups have been studied and tested for caspase inhibition with much success.[10] The incorporation of a pyridine ring on the amide nitrogen was also proposed due to the success of the pyridoxymethyl ring on the C-5 extended sulfonamide.

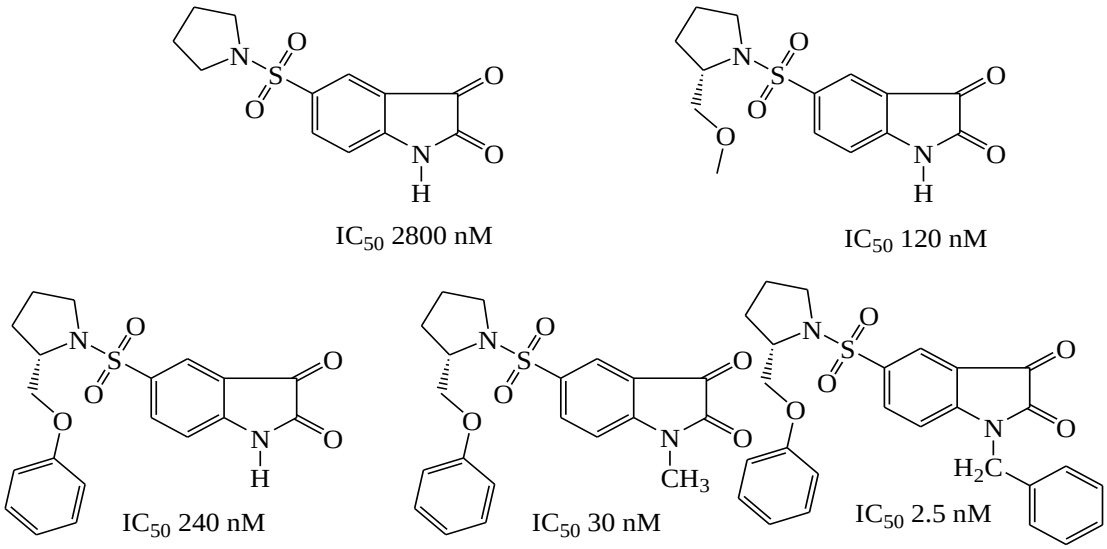

Figure 5

A comparison between the phenoxymethyl analogue and the pyridoxymethyl analogue showed increased inhibition properties for the pyridine derivatives as shown in **Table 1**.

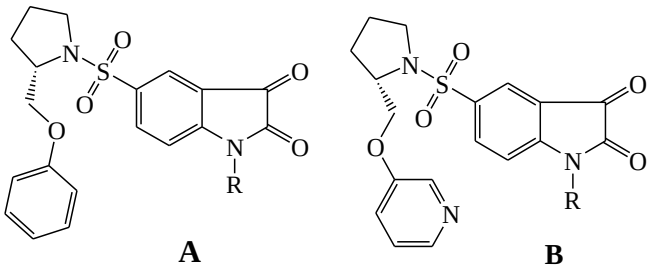

A **B**

Table 1: Comparison of Phenoxymethyl and Pyridinoxymethyl Rings

R	IC_{50} (nM) Phenoxymethyl Ring (A)	IC_{50} (nM) Pyridinoxymethyl Ring (B)
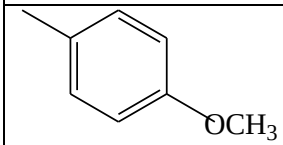	14.5	5.2
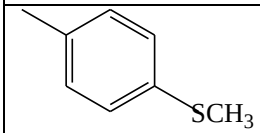	12.4	3.9
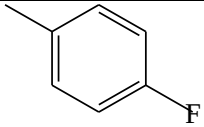	12.1	4.4

A summary of the SAR study is presented in **Figure 6.** By having two main functional sites, the WashU investigators were able to vary three different regions on their inhibitors.

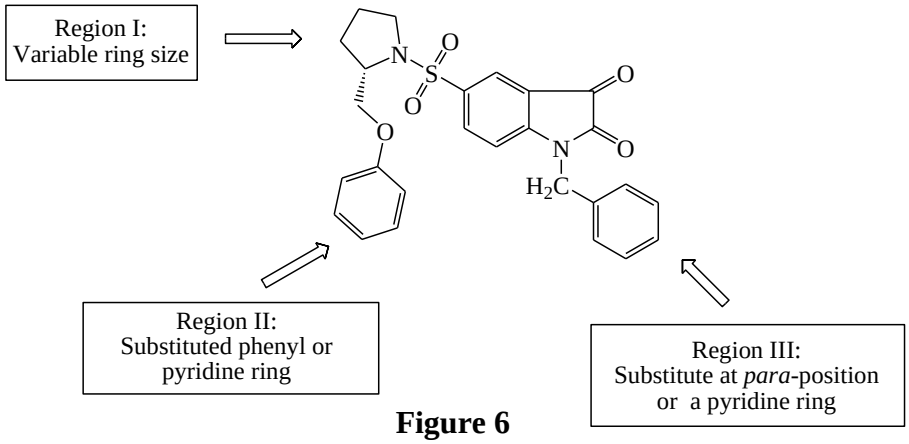

Figure 6

The WashU group also built upon their own isatin sulfonamide scaffold by adding a third point of variation on the C-3 carbon of isatin.[10] By having an EWG at the C-5 position and a group on the amide nitrogen, this group was able to functionalize the C-3 carbonyl to form an isatin Michael acceptor (IMA) featuring a dicyano vinyl group as the acceptor. By adding the dicyano group to the C-3 position, the specificity of the inhibitor towards the effector caspases changed. For example, **Figure 7** shows the IC_{50}'s of two inhibitors, one with a carbonyl at C-3 and the other with the IMA at C-3.

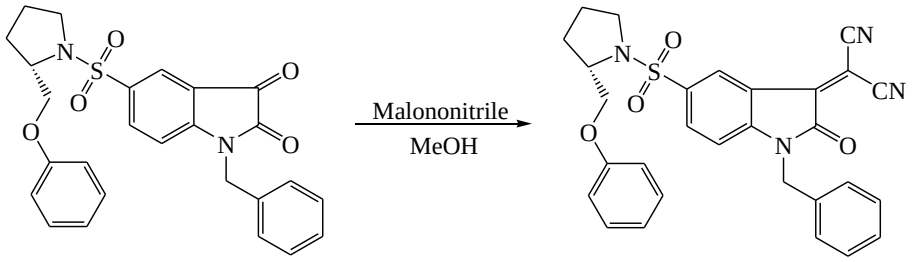

Caspase-3: 14.5 ± 1.6 nM
Caspase-6: > 5,000 nM

Caspase-3: 27.8 ± 2.5 nM
Caspase-6: 918 ± 151 nM

Figure 7

Based on the IC_{50}'s of the two inhibitors in **Figure 7,** the IMA favored caspase-6 while the isatin analogue was more potent against caspase-3.[10] Such differentiation is important due to the fact that different diseases carry out apoptosis via different caspases. Alzheimer's disease executes apoptosis via caspase-3 while Huntington's disease operates mainly via caspase-6. However, as designed, there is a limitation to the IMA as regards to further development in that the C-3 position cannot be further functionalized beyond the two requisite cyano groups.

Previous to this, Dr. Edward Brush of Bridgewater State College introduced a Michael acceptor onto an oxindole scaffold at the C-3 position, creating 3-methyleneoxindole (**9**).[11] The methylene oxindole scaffold **10** is very similar to isatin (**7**), with the exception of a CH_2 group present at the C-3 position rather than a carbonyl.

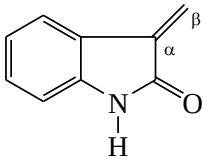

9

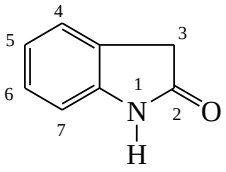

10

Since the activated cysteine residue of the caspase can be considered a "soft" nucleophile, the corresponding "soft" β-position of methylene oxindole may allow such substrates to act as effective Michael acceptors for the inhibition of caspases as well as other cysteine proteases.

More recently, a group in Australia discovered a new mechanism of action between their peptide inhibitors and caspase-1.[12] As mentioned earlier, the activated cysteine thiol acts as a nucleophile, which attacks at the carbon of the warhead bearing a leaving group and covalently bonds to the inhibitor at that site. Löser *et al.* showed that it

was not necessary to have an electrophilic warhead on the peptide inhibitor to have inhibitory capabilities. They instead used a variety of secondary and tertiary amines as the warhead, as shown by the secondary amine bearing a phenol ring on the C-terminal side of the modified P_1 aspartic acid group in structure **11**. By doing this, they were able to show that covalent interactions between key subsites on caspase-1 and the inhibitor can produce potent, reversible inhibitors.[12] This work is also important due to the fact that secondary and tertiary amines are stable *in vivo*, meaning that the inhibitor has high bioavailability and stability.

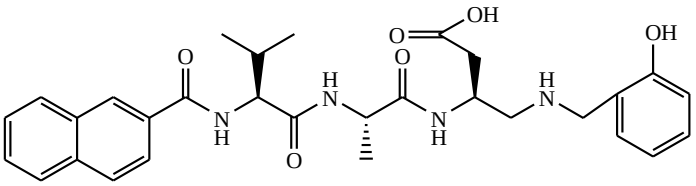

11

When tested against caspase-1, it was found that the amine nitrogen was positioned in the substrate binding groove between the Cys 285 and the His 237 residues, and the 2-hydroxybenzylamine was positioned in the S_1' subsite.[12] Shown in **Figure 8** is a model conformation of **11** in the active site of caspase-1. This figure demonstrates that there is appreciable hydrogen bonding between the 2-hydroxybenzylamine and the Asp 288 residue in the S_1' subsite, and also between the amine nitrogen and the His 237 residue as shown by the dashed lines.

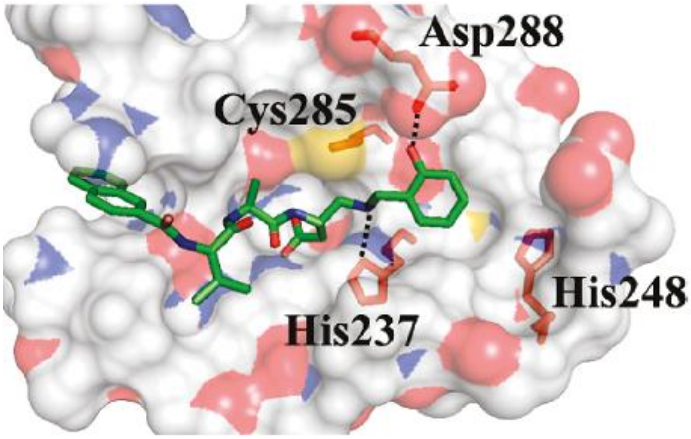

Figure 8

This research performed by Löser *et al.* is significant because it proposes that hydrogen bonding between the inhibitor and the binding site of the caspase greatly influences the inhibition capabilities of the inhibitor. Accordingly, substituent groups with available electrons such as hydroxyl and methoxy groups could be used as possible groups on caspase inhibitors, contrary to prior belief.

OBJECTIVES

Based on the previously stated research findings, the present project was to develop, synthesize and characterize caspase inhibitors using a combinatorial approach. As described earlier, SKB and the WashU group prepared a series of inhibitors using an isatin scaffold with two points of variability. While more recently the WashU group initiated studies on Michael acceptor based caspase inhibitors derived from such isatins, such inhibitors also possess just two sites of variability. The goal of this project is to develop benzylidene oxindole derivatives bearing three sites of diversity as potential Michael acceptors for caspase inhibition. A structural summary of the previous and proposed families of small molecule caspase inhibitors are shown below in **Figure 9**.

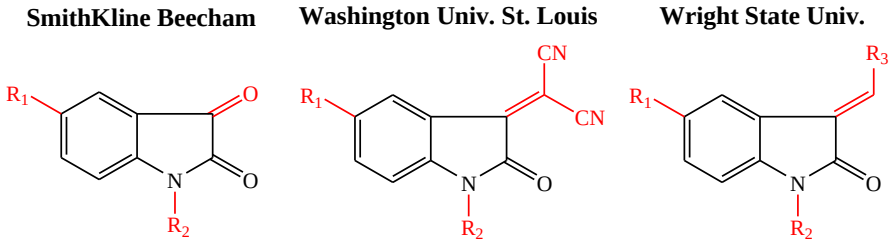

Figure 9

To synthesize such a combinatorial library of oxindole derived potential Michael acceptors for caspase inhibition, it was deemed necessary to develop a plan based on the functionalization and utilization of both oxindole and isatin derivatives (*vide infra*). The first step in the anticipated series of reactions would involve the addition of different functionalities to the C-5 position of these substrates. To that end, the nitration of the C-5 positions of isatin and oxindole were conducted, according to **Schemes 2**[13] and **Scheme 3**.[14]

Scheme 2

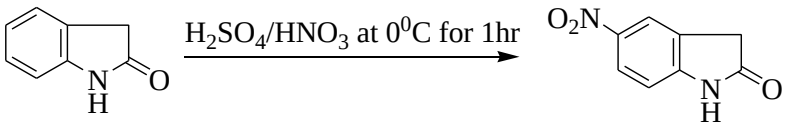

Scheme 3

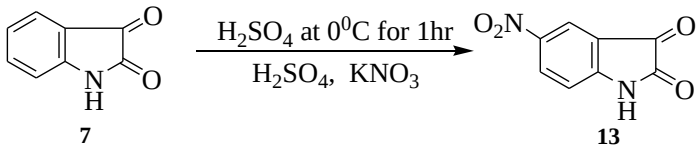

The nitration procedure follows an Electrophilic Aromatic Substitution (EAS) mechanism.[15] In the EAS mechanism, sulfuric acid protonates nitric acid, giving off water as a byproduct and thereby generating the actual nitronium ion electrophile. The EAS mechanism, which is the same mechanism followed for the nitrations of both **7** and **10** is shown in **Scheme 4**.

Scheme 4

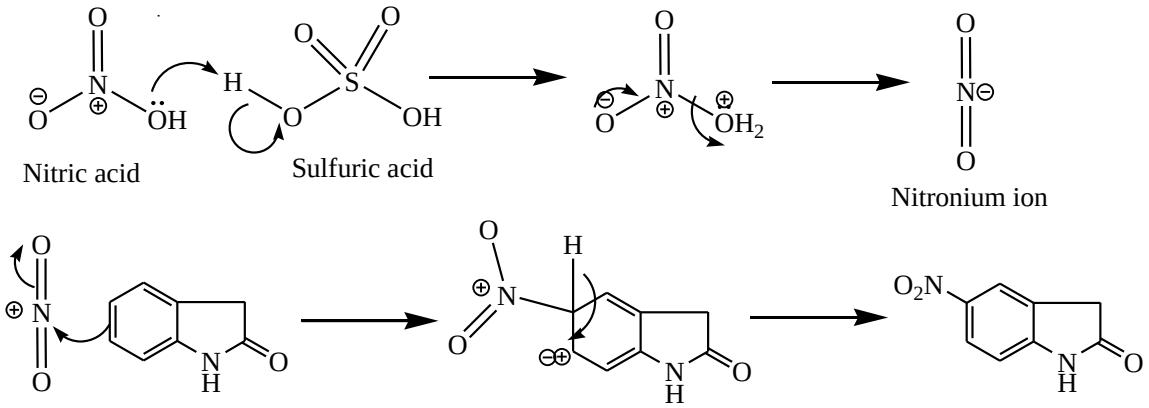

Secondly, in place of the potentially reducible nitro group, a sulfonamide at the C-5 position was desired. To this end, both oxindole and isatin were treated with

chlorosulfonic acid to initially produce sulfonyl chloride derivatives, prior to treatment with the appropriate amines as shown in **Scheme 5**[16] and **Scheme 6**[17].

Scheme 5

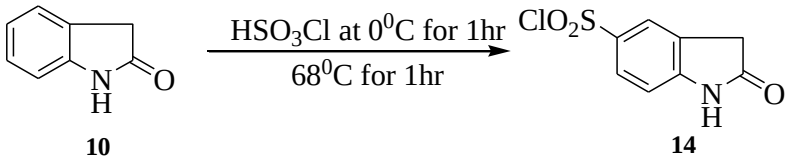

10 **14**

Scheme 6

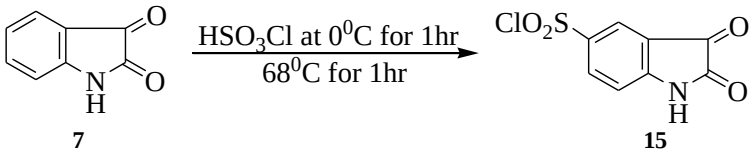

7 **15**

The necessity of functionalizing both oxindoles and isatins stems from the fact that oxindole cannot be alkylated regioselectively since it produces an ambident anion which affords a mixture of N-alkyl and 3-alkyl derivatives. Thus, in order to secure N-alkylated oxindoles before the aldol reactions necessary to produce benzylidene oxindoles, such alkylations must be performed at the isatin oxidation level. This N-alkylation must be performed before the reduction of the C-3 carbonyl of **7** to the CH_2. When the 5-substituted isatin is reduced to a 5-substituted oxindole, it will have two possible points of alkylation, the amide nitrogen and the α-carbon. **Scheme 7** shows the possible outcomes of an alkylation reaction on 5-substituted oxindole.[18]

Scheme 7

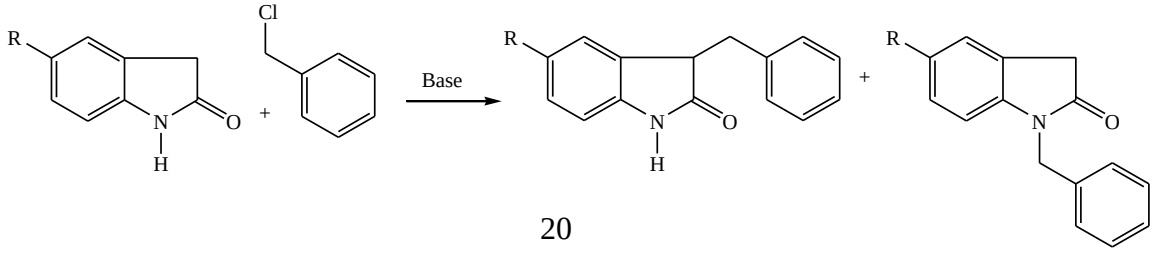

Thus, in order to secure N-alkylated oxindoles before the aldol reactions necessary to produce benzylidene oxindoles, such alkylations must be performed at the isatin oxidation level. **Scheme 8** shows the process that will be used for the N-alkylation of isatin. Various alkyl groups will be used to determine the best possible combination of functional groups for optimum inhibition.

Scheme 8

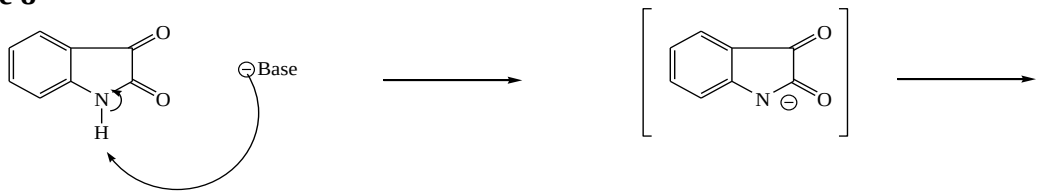

In the first step the base abstracts a proton from nitrogen

Secondly, the highly conjugated isatin anion is formed

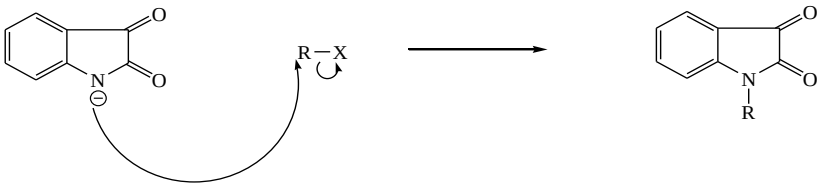

The next step involves the nucleophilic attack on the alkyl halide reagent

Final N-alkylated isatin product

Thus, upon C-5 functionalization, the oxindole can be treated directly with an aldehyde to afford the desired alkylidene oxindole, or if N-substitution is desired the corresponding N-alkylated isatin can be reduced to the oxindole by Wolff-Kishner reduction of the C-3 carbonyl using 80% hydrazine hydrate as the reducing agent.[19] The reaction scheme is shown in **Scheme 9**.

Scheme 9

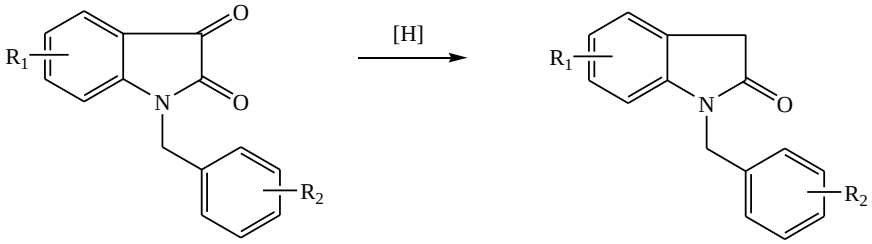

This step will also be desirable due to the cost difference between isatin and oxindole. Isatin is much cheaper than oxindole, making it the more affordable and the economical option for the experiments. The mechanism[20] for the Wolff-Kishner reduction is shown in **Scheme 10**.

Scheme 10

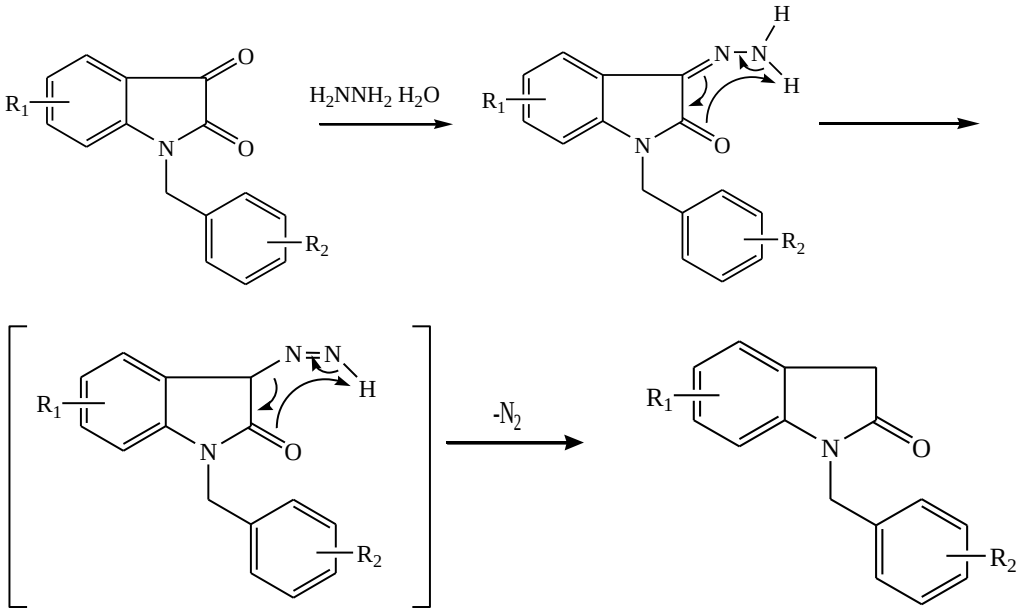

After reduction of the N,5-disubstituted isatin to an N,5-disubstituted oxindole, an aldol condensation is envisioned. The aldol condensation[21] is a reaction between an α-carbanion and an aldehyde. A weak base is used to abstract the α-H and the resulting enolate anion can then act as a nucleophile to attack the carbonyl of the aldehyde followed by a loss of water. The mechanism for this reaction is shown in **Scheme 11**.[22]

Scheme 11

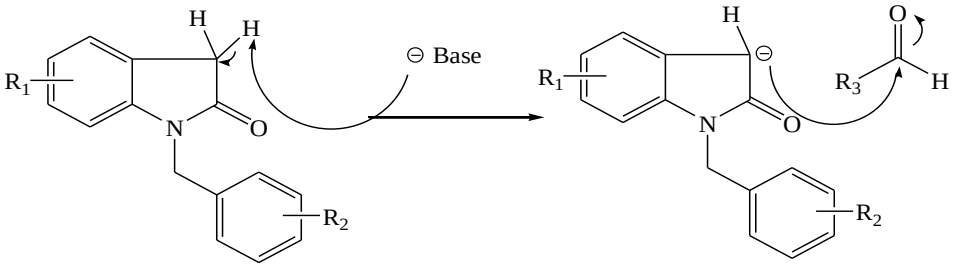

Strong base abstracts a proton a to the carbonyl

Nucleophilic attack on the aldehyde carbonyl breaking the double bond

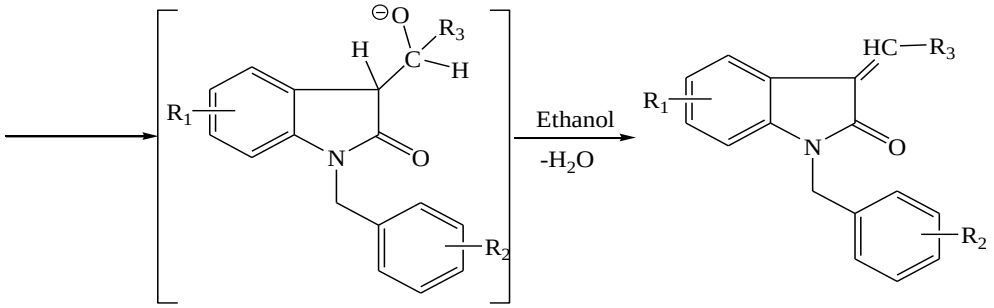

-O abstracts proton from ethanol followed by dehydration

RESULTS AND DISCUSSION

Initial attempts at securing 5-chlorosulfonylisatin involved heating isatin (**7**) in chlorosulfonic acid at 70 °C according to a literature procedure.[17] However, the identity of this compound was recently called into question by the GSK[8] group, who instead isolated a high yield of the *gem*-dichloro derivative (**16b**) as seen in **Scheme 12**.

Scheme 12

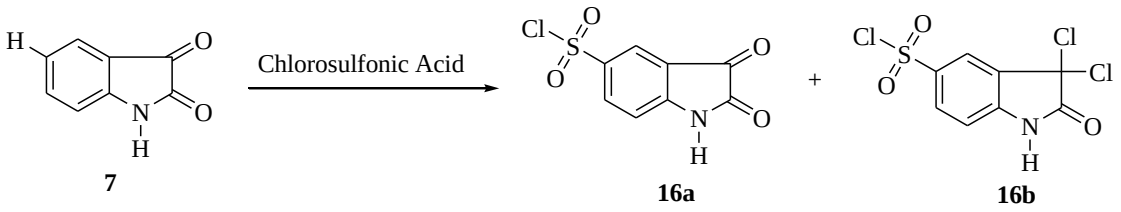

7 **16a** **16b**

In our experiment, a melting point was performed on the product and it was found to be 137-140°C. Isatin has a melting point of ~201°C, which provides evidence that the product is different from the starting material. Unfortunately, the literature melting points for 5-chlorosulfonylisatin vary greatly, the earliest preparation in which the product was recrystallized from acetone-benzene was reported to have a melting point of 150-152 ^{o}C,[17] whereas more recent approaches involving treatment of 5-isatinsulfonic acid sodium salt with phosphorus oxychloride in tetramethylene sulfone reported a product with a melting point of 188-190 ^{o}C.[9] Since we were unable to directly chlorosulfonate isatin, and in light of the recent commercial unavailability of 5-isatinsulfonic acid sodium salt, it was decided to abandon further investigations into the study of sulfonamide isatins and their reduction to oxindoles.

Attention was then focused on the N-alkylations of isatin using KF/alumina as a novel base and different alkylating agents.[23] Whereas the literature protocols for N-

alkylation normally involve the use of CaH_2 in DMF solvent, the present protocol, employing acetonitrile as the solvent and KF/alumina as the base, would give an opportunity for a novel approach to this well studied N-alkylation reaction. The reaction was performed according to **Scheme 13** and the data associated with these experiments are shown in **Table 2**.

Scheme 13

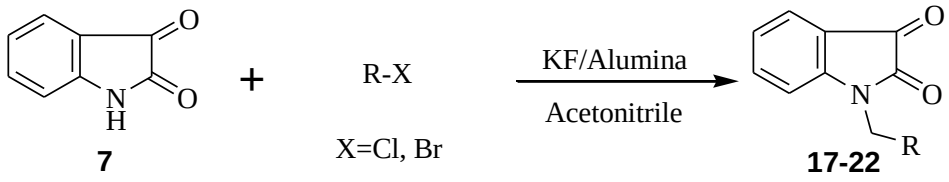

Table 2: N-Alkylations of Isatin using KF/Alumina or CaH_2					
Compound #	**Base**	**R**	**Experimental Melting Point (°C)**	**Literature Melting Point (°C)**	**% Yield**
17	KF/alumina	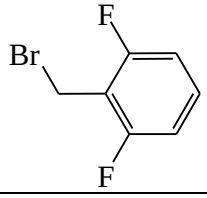	178-185	N/S*	37.1
18	KF/alumina	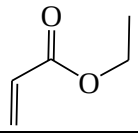	Liquid	N/S	N/A
19	KF/alumina	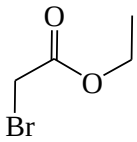	190-197	132-133[23]	Starting Material
20	KF/alumina	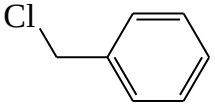	196-199	133-134[23]	Starting Material
21	CaH_2	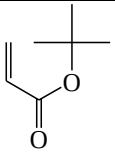	Liquid	N/S	24.9

22	CaH_2	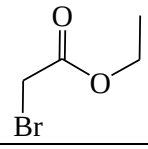	124-128	132-133[23]	38.3
23	CaH_2	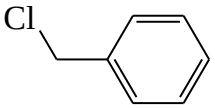	134-139	133-134[23]	15.1

*N/S= product has not been synthesized before in the literature.

Unfortunately, the reactions performed were largely unsuccessful, with many of the reactions simply returning unreacted starting material, as proven by the melting points and their similarities to the melting point of **7**. The data presented in **Table 2** indicates that N-alkylations using KF/alumina are not very promising. The reactions performed to prepare compounds **18** and **21** involved attempted Michael type acceptors instead of alkyl halides. For the preparation of compounds **22** and **23**, the literature protocol involving CaH_2 and DMF was used. From **Table 2**, the experimental melting points and the literature melting points for compounds **22** and **23** are very similar, showing that the products are in fact the predicted ones, despite the fairly low yields. Considering that the major goal of this research was the preparation of about 10 mg of a compound for screening, low yields were not considered an issue throughout this program of research because biological activity took priority over yield. If the compound was screened and found biologically active, then further experimentation would be done to increase the overall yield.

Having decided to abandon the C-5 sulfonamide moiety, the less desirable nitro group was then chosen as a representative EWG for our studies. Thus, a nitration procedure was performed on isatin **7** and the melting point of the product was used to to compare it with the literature value published by SKB,[8] as shown in **Scheme 14**.

Scheme 14

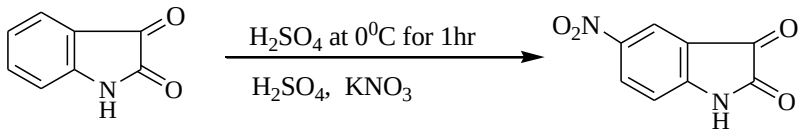

Many of the procedures found in the literature for the nitration of **7** use fuming nitric acid,[24,25] which was deemed undesirable due to lab safety considerations. An alternate procedure was found which employs potassium nitrate and concentrated sulfuric acid.[14] Using this procedure, a solution of potassium nitrate and sulfuric acid was first prepared and cooled to 0 ^{o}C in an ice bath. A second solution of isatin and sulfuric acid was prepared and added dropwise to the aforementioned potassium nitrate solution over a period of 1 hr, making sure that the reaction temperature did not exceed 5 °C. The reaction mixture was then poured over ice and the solid collected via vacuum filtration. The melting point of the product was 249-252 °C, which was very close to the literature melting point of 252-254 °C.[14] Since this compound is known and had been shown by SKB to be active as a caspase inhibitor, a sample of **13** was sent to Dr. Thomas L. Brown for screening to compare the results using the Brown protocol to the SKB results. Since the N-alkylation reactions on **7** were not as successful and an N-methyl or N-benzyl derivative could not be produced, it was not expected that the N-unsubstituted isatin **13** would be highly active, and in the event it was found inactive in the Brown protocol at concentrations of up to 100 μM. Additionally, it was also decided to test compounds **7** and **10** to determine if any activity might be attributable to the scaffolds themselves, and expectedly they were found inactive.

Since at the moment it appeared that isatin derivatives with known activity were likely to show no activity in the Brown protocol, it was decided to focus on the benzylidene oxindoles described earlier by analogy to the Michael acceptor prepared by Dr. Edward Brush but with the potential for more sites of variability. Recalling that the SKB[8] and WashU[10] inhibitors had a maximum of two points of variability, the proposed benzylidene oxindoles have the advantage of having three readily accessible points of variability with the potential to tune potency and selectivity amongst various caspases.

Deciding to employ oxindole as a potential scaffold for caspase inhibitors, a nitration procedure was then performed to add a $-NO_2$ group at the C-5 position. Even though this group is known to be reduced *in vivo*, it was decided to prepare some analogs bearing this functionality and if activity was found due to the presence of certain groups at the C-3 or N-position(s), another more suitable EWG at C-5 could be substituted. Therefore, compound **12** was prepared by nitration of **10** at 0 ^{o}C employing nitric acid/ sulfuric acid as shown in **Scheme 15**.[13]

Scheme 15

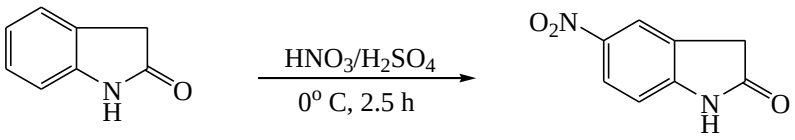

10 **12**

The product was recrystallized using a 50% acetic acid: water solution affording an overall yield of 85% after recrystallization. The melting point was determined to be 244-245°C which compares well with the literature melting point of 240-241°C, concluding that the product synthesized was indeed **12**.[13] Additionally, the formation of the product was confirmed by GC/MS and NMR spectroscopic analysis. With the

oxindole bearing a strongly EWG at the C-5 position in hand, aldol condensations using several different aldehydes and **12** were then conducted to functionalize the C-3 position according to **Scheme 16**.

Scheme 16

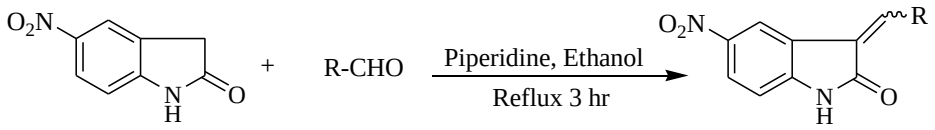

In a typical procedure, a reaction mixture of **12** (1 equiv), aldehyde (1.2 equiv), and piperidine (0.1 equiv) in ethanol was stirred at 90 ^{o}C for 3-5 h.[21] After the mixture cooled, the precipitate was filtered, washed with cold ethanol, and dried to give the target compounds. The aldehydes employed are shown in **Table 3**.

Table 3: Aldol Condensations using 5-Nitroindolin-2-one

Compound #	R	Experimental Melting Point (°C)	Literature Melting Point (°C)	*E* or *Z* Isomer	Biological Activity
24	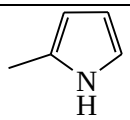	>295	308-310[32]	*Z*	negative
25	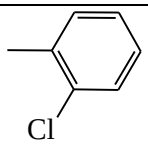	269-271	N/S	*E*	N/T
26	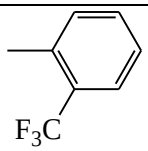	218-221	N/S	*E:Z* 93:6	negative
27	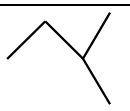	231-234	N/S	*Z*	N/T

28	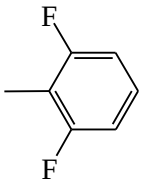	251-255	N/S	*E*	negative
29	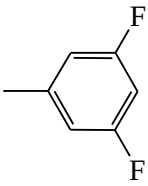	301-306	N/S	*E:Z* 75:25	negative

*N/T= product not tested for biological activity *N/S= product has not been synthesized before in the literature

The *E*:*Z* ratio of isomers in **Table 3** were determined by GC/MS analysis. Upon aldol condensation and spontaneous dehydration, the resultant benzylidene oxindoles can exist in either the *E* or *Z* conformation (or a mixture of both). The ^{1}H NMR spectrum of each compound was examined very closely for subtle indicators that predict and confirm the configuration of each product. The literature[26] shows that the chemical shifts for the C-2' and the C-6' protons in the *Z* isomer are more downfield (7.85-8.53 ppm) than the C-2' and the C-6' protons in the *E* isomer (7.45-7.84 ppm). In general, the C-2' and the C-6' (*ortho*) protons will be shifted downfield relative to the vinyl proton in the *Z* isomer, and the opposite is true for the *E* isomer. The different structures for the *E* and *Z* isomers are shown in **Figure 10**.[27] To determine if the products are accurately predicted, ^{1}H and ^{13}C NMR spectroscopic analyses were performed. All of the spectra generated were analyzed and expanded using SpinWorks 3.1.

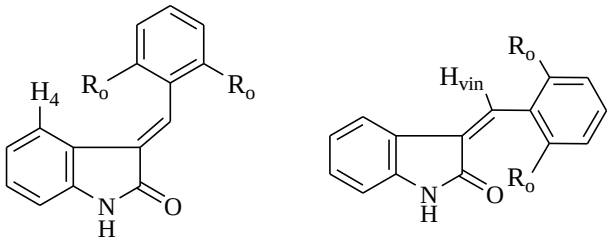

E Isomer *Z* Isomer

Figure 10

There are several factors that can act to determine whether the compound will be predominantly in the *E* or the *Z* isomer. Electrostatic interaction between the substituents on the C-3 benzylidene ring and the C-2 carbonyl will cause the ring to be in the *Z* isomer, while electrostatic repulsion will cause the ring to move into the *E* isomer form.[27] Also, hydrogen bonding between the substituents at the different positions on the C-3 benzylidene ring and the C-2 carbonyl would also cause the products to favor the *Z* over the *E* configuration.[27]

The compounds that were of most interest were those containing the 2,6-difluorobenzaldehyde moiety, due to structural similarities to the Q-VD-OPh model inhibitor. Compound **28**, along with several other products from **Table 3** were sent to our collaborator Dr. Thomas L. Brown for biological screening. The biological assay is performed to verify whether the compound being tested inhibits apoptotic cell death or not. The tests conducted were blind tests, meaning that the researchers doing the screening did not know what the compounds were; this eliminates any bias that may occur. The screening was also done by different people at different times and all received the same results. The gel for compound **28** is shown in **Figure 11.**

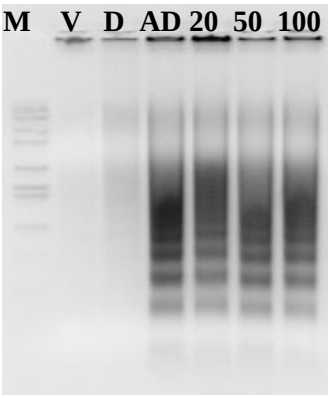

8 x 10^6 cells/ml of Jurkat cells
M- Marker
V-Vehicle: 10µL DMSO + 10µL Methanol
D- Drug only: 10µL 50mM **28** + 10µL Methanol
AD- Actinomyocin D only: 10µL of 1µg/µL Actinomyocin D + 10µL DMSO
20- 10µL of 20mM **28** + 10µL of 1µg/µL Actinomyocin D
50- 10µL of 50mM **28** + 10µL of 1µg/µL Actinomyocin D
100- 10µL of 100mM **28** + 10µL of 1µg/µL Actinomyocin D

Figure 11

The "M" channel is the DNA marker channel, which shows the DNA strands being tested. The "V" channel contains the solvent and the cells being tested only and no compound **28**. The Drug (D) channel is compound **28** in methanol along with the cells being tested. The "AD" channel contains cells that are treated with the Actinomycin D protein, which is a pro-apoptotic protein secreted from the mitochondria. The channels that are marked with 20, 50 and 100 are the concentrations that the compound is being tested at. The dark bands translate to inactivity, which also means the cells used for this assay, which were Human Jurkat T cells (Type 2 cells), underwent apoptotic cell death even at high concentrations (such as 100µM) of potential inhibitors.

While it was deemed important to determine the relative inhibitory properties of compound **28** possessing the 2,6-difluorophenyl moiety resembling the warhead of Q-VD-OPh, it was also thought interesting to examine the activity of compound **29** the 3,5-

difluoro substitution pattern, as this was thought to enhance the Michael acceptor properties of the substrate. Unfortunately, compound **29** proved insoluble under the screening conditions, so that proof of this hypothesis could not be achieved.

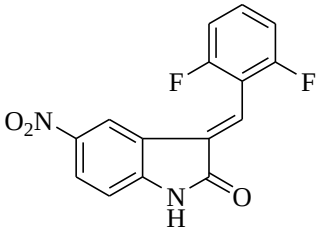

28

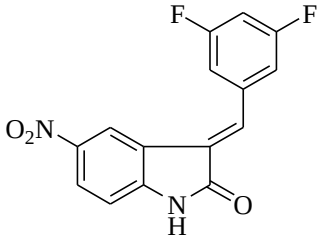

29

It is also interesting to note that 5-nitroisatin (**13**) which was found active against caspase-3 by GSK, showed no activity in the WSU screen (gel not shown). Although there are significant differences between the literature IC_{50} value and the value determined by the Brown protocol, this was determined inconsequential as we could establish a relative scale of activity for our compounds in any case.

After a review of the screening results and careful interpretation of those results, a change in strategy was put into effect. Since a $–NO_2$ group demonstrated no clear advantage and could be reduced to a toxic amine, it was decided to simply study the C-5 unsubstituted oxindoles so as to determine the role of the group at C-3. Previously, Löser *et al.* had demonstrated that there was no need for an electrophilic functional group on the inhibitor for it to be active.[12] It was then decided to perform aldol condensations on oxindole (**10**) using several different aromatic aldehydes with a range of electron withdrawing as well as electron donating substituents, especially those which might have available electron lone pairs for possible hydrogen bonding effects. Thus**,** 3-substituted

indolin-2-ones were prepared by condensing indolin-2-one and aldehydes in the presence of a base. **Scheme 17** shows the reaction procedure used for the aldol condensations.[21]

Scheme 17

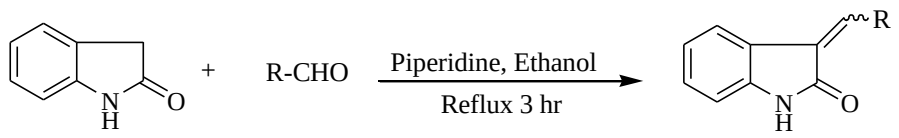

10 **30-40**

The first procedure attempted used 10 equivalents of the base piperidine according to one literature procedure.[16] Unfortunately, the yields for these reactions were very low at only ~20%. The second procedure used to make the same compounds used only 0.1 equivalents (a catalytic amount) of piperidine and had much higher yields, approximately 80%.[21] Several aldehydes were used following these procedures and their products are listed in **Table 4**.

Table 4: Aldol Condensations using 5-Indolin-2-one and Aldehydes

Compound #	R	Experimental Melting Point (°C)	Literature Melting Point (°C)	*E* or *Z* Isomer	Biological Activity
30	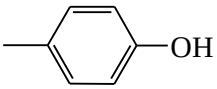	298-301	300+[28]	*E*	negative
31	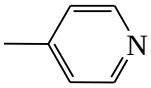	226-229	225-226[29]	*E:Z* 9:91	active
32	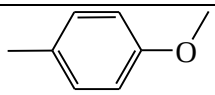	152-155	155-156[18,30]	*E:Z* 94:6	active
33	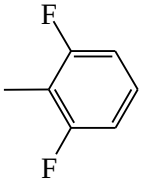	213-218	N/S	*E*	negative

34	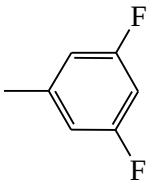	202-205	N/S	*E:Z* 92:8	negative
35	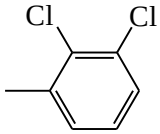	263-265	N/S	*E:Z* 73:27	N/T
36	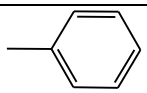	172-175	175-176[30,31]	*E*	N/T
37	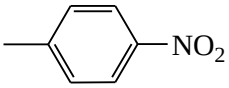	251-252	252-253[30]	*Z*	negative
38	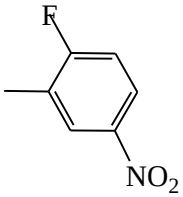	199-201	N/S	*Z*	N/T
39	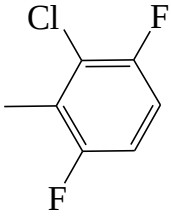	207-211	N/S	*E*	N/T
40	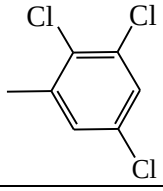	268-270	N/S	*E:Z* 90:10	N/T

*N/T= product not tested for biological activity *N/S= product has not been synthesized before in the literature

The *E*:*Z* ratio of isomers in **Table 4** were determined by GC/MS analysis. In assigning *E* or *Z* configuration to the compounds in the table above, the NMR analysis conducted on compound **30**, which contains a hydroxyl functionality at the C-4' position on the C-3 benzylidene ring will be used as an example. In the ^{1}H NMR spectrum, the C-2' and C-6' (*ortho*) protons are displayed as a doublet signal centered at 7.61 ppm while

the vinyl proton appears as a singlet at 7.31 ppm. Therefore, the *ortho* protons are further downfield than the vinyl proton, allowing assignment as the *E* configuration by the NMR considerations described earlier. This ^{1}H NMR spectrum analysis was applied to all of the compounds synthesized throughout this research to determine *E* or *Z* configurations.

Several of the compounds synthesized in **Table 4** were tested for biological activity, including compound **33** (possessing the 2,6-difluorophenyl moiety of Q-VD-OPh), the result of which is shown in **Figure 12**. The dark bands in the 10, 20, 50 and 100 channels in **Figure 12** show that compound **33** is inactive even at the highest concentration.

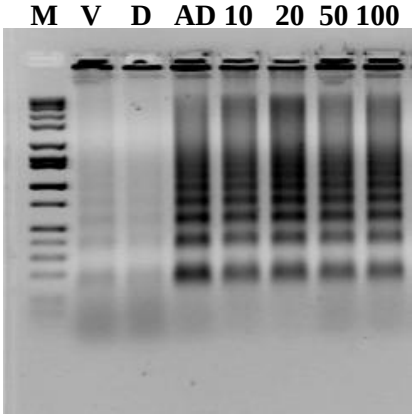

1x 10^{7} cells/ml of Jurkat cells
M- Marker
V-Vehicle: 10µL DMSO + 10µL Methanol
D- Drug only: 10µL of 50mM **33** +10µL Methanol
AD- Actinomyocin D only: 10µL of 1ug/ µL Actinomyocin D + 10µL Methanol
10- 10µL of 10mM **33** + 10µL of 1µg/µL Actinomyocin D
20- 10µL of 20mM **33** + 10µL of 1µg/µL Actinomyocin D
50- 10µL of 50mM **33** + 10µL of 1µg/µL Actinomyocin D
100- 10µL of 100mM **33** + 10µL of 1µg/µL Actinomyocin D

Figure 12

The structure for **33** was confirmed by ^{1}H and ^{13}C NMR spectroscopic analysis. To do this, the core structure (compound **10**) was analyzed first using ^{13}C NMR spectroscopy. The ^{13}C NMR **Figure 13** shows eight signals that correspond to all eight carbons in **10**.

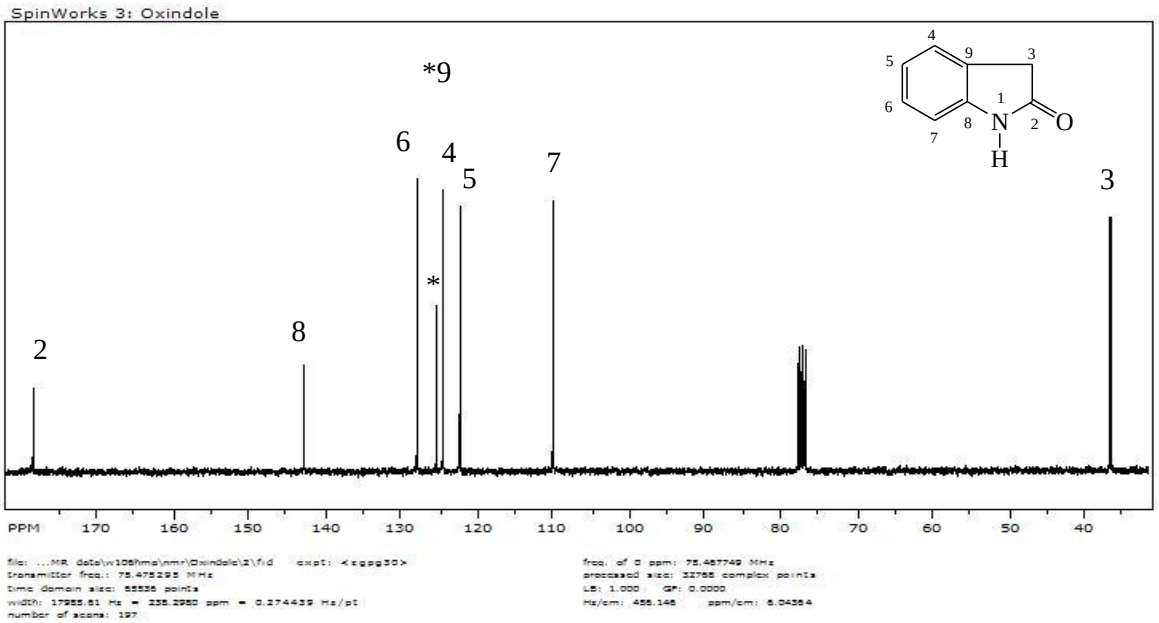

Figure 13

The solvent signal, $CDCl_3$, appears at ~77 ppm. The C-2 amide carbonyl appears in the spectrum at 178.59 ppm. The C-3 methylene signal appears in the aliphatic region at 36.39 ppm. The aromatic region, approximately 110-150 ppm, contains six signals for the remaining six carbons on **10**. To distinguish the aromatic CH carbons from the quaternary carbons, a ^{13}C DEPT 90 NMR spectrum was acquired on **10**. Quaternary carbons do not appear in any of the ^{13}C DEPT subspectra, meaning that the spectra should only contain four signals in the aromatic region that correspond to the four aromatic CH's, which was the case. The C-8 carbon appears further downfield at 142.84

ppm, due to its proximity to the amide nitrogen. Also, the C-9 carbon is an aromatic, quaternary carbon. When the ^{13}C NMR of **10** is compared to the ^{13}C DEPT 90 spectrum, a peak at 125.37 ppm disappears in the ^{13}C DEPT 90 spectrum, meaning that the signal corresponds to the quaternary C-9 carbon. The remaining four aromatic CH carbons are as follows; C-4 at 124.50 ppm, C-5 at 122.28 ppm, C-6 at 127.91 ppm and C-7 at 109.99 ppm. These values are consistent with the values stated in the literature.[33,34]

After performing an aldol condensation reaction using 2,6-difluorobenzaldehyde, the product, (*E*)-3-(2,6-difluorobenzylidene)indolin-2-one (**33**), was also analyzed using ^{13}C NMR spectroscopy, using the signals from **10** as the core scaffold. **Figure 14** shows the ^{13}C NMR spectrum of **33**.

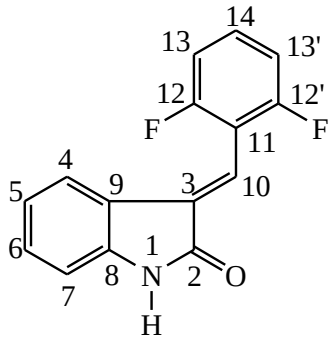

33

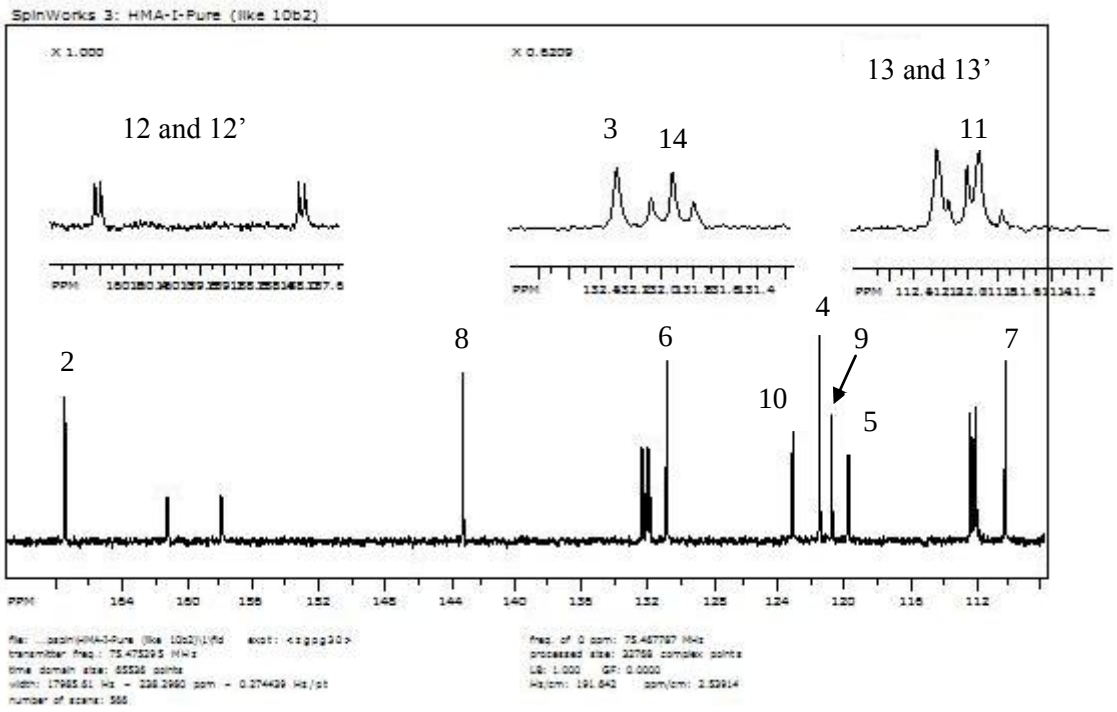

Figure 14

Based on the structure of the product, there are 13 different carbon atoms that correspond to the 13 signals observed. The solvent used for this sample was DMSO-d_6 and that signal appears at ~39.5 ppm. As can be seen from **Figure 14**, the C-2 carbonyl carbon has shifted upfield to 167.53 ppm. The spectrum shows a very broad doublet of doublet peaks at ~161 and ~158 ppm, which correspond to carbons labeled C-12 and C-12'. This broadening of the doublet peaks is due to the fluorine atoms, the first atom splitting the carbon spectrum to create a doublet while the second fluorine splits the spectrum again, creating a doublet of doublets. The carbon labeled C-8 does not change position in the spectrum even after the reaction; it still appears at 143.23 ppm. The C-3 carbon, however, shifts dramatically downfield into the olefinic region, since it began as a methylene carbon and became a double bonded quaternary carbon, which now has a

signal at 132.29 ppm. There is also a triplet signal centered at 131.93 ppm, which corresponds to the carbon labeled C-14. The C-14 carbon is experiencing splitting by the fluorine atoms on the benzylidene ring, creating a triplet signal.

The C-7 carbon remains relatively unchanged with a signal at 110.12 ppm in **Figure 14**. Also, a signal appears at 120.70 ppm in the ^{13}C NMR that does not appear in the ^{13}C DEPT 90 NMR spectrum and this has been assigned to C-9 due to its quaternary nature and its aromaticity, which is fairly close to the oxindole value. The ^{13}C DEPT 90 NMR spectrum shows the CH peaks that are in the aromatic region. The carbons from the original structure of **10** in **Figure 13** are relatively in the same position, with the C-4 signal showing at 121.46 ppm, the C-5 signal appearing at 119.71 ppm and the C-6 carbon signal emerging at 130.80 ppm. The carbon labeled C-10 is a CH carbon which appears in both spectra as a triplet at 123.09 ppm. This splitting of the C-10 signal is also due to its proximity to the fluorine atoms. Further, the C-11 signal is split into a triplet and is overlapped within the C-12 and C-12' signal, with its center peak showing at ~112 ppm.

It was very discouraging to see that compound **33** was inactive, since the initial expectation had been that the difluorophenyl group from Q-VD-OPh would be a successful addition to the active inhibitor library. The active compound **X** though, was created by pure accident. Originally, using compound **33** as the starting material, it was decided to nitrate the compound assuming that addition of the nitro group would occur exclusively or predominantly at the C-5 position although there was no literature precedent.[13] **Scheme 18** shows the reaction performed on **33** and the predicted product.

Scheme 18

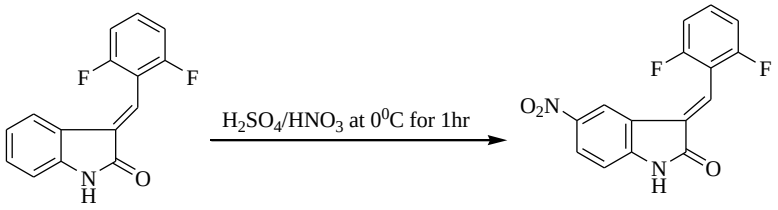

33 **28**

If the nitration had occurred on the C-5 position, then compound **28** would be the final product. However, the product obtained from the nitration of benzylidene oxindole demonstrated significant cell death inhibition. From the data in **Table 3**, the expected product **28** demonstrated no inhibition of cell death, it was therefore assumed that **28** could not be the nitrated compound obtained, and that nitration had occurred elsewhere on the molecule, perhaps even on the difluorophenyl ring. The reaction and its possible product(s) are shown in **Scheme 19**. Moreover, there is a mysterious byproduct that forms during this procedure that has a molecular weight of 282 *m/z* by GC/MS analysis, while the starting material **33** has a molecular weight of 257 *m/z.* Therefore, there is only one nitro group adding to the compound, giving it a total molecular weight of 302 *m/z*. In the case of the byproduct, the mass difference from the expected product indicates a possible loss of a fluorine atom perhaps by some nucleophilic aromatic substitution process. The initial screen involved testing of a sample consisting of approximately equal amounts of **X** and its defluorinated byproduct. Although it was not common practice to screen impure mixtures, failed initial attempts to purify the sample and in the interests of time, an answer as to the potency of the 2,6-difluorophenyl group was needed and if it were highly active, even a mixture would demonstrate cell death inhibition.

Scheme 19

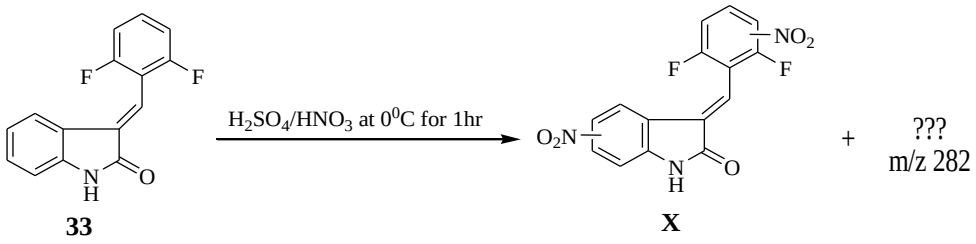

The biological assay performed on compound **X** is shown in **Figure 15**. As can be seen in **Figure 15**, compound **X** was 100% active at 100 µM and about 50% active at 50 µM, even in its impure state.

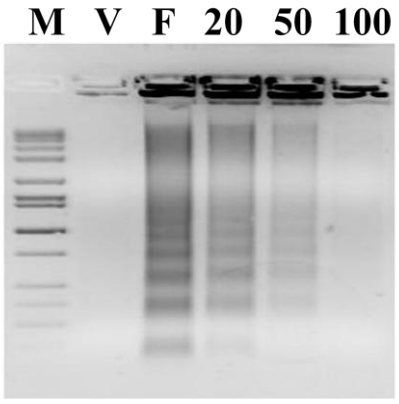

8.45 x 10^6 cells/ml of Jurkat cells
M- Marker
V-Vehicle: 10µL DMSO
F- α Fas only: 2µL of α Fas (clone C-11) 100ng/mL[Final] + 10µL DMSO
20- 10µL of 20mM **X**+ 2µL of α Fas (clone C-11) 100ng/mL[Final]
50- 10µL of 50mM **X** + 2µL of α Fas (clone C-11) 100ng/mL[Final]
100- 10µL of 100mM **X** + 2µL of α Fas (clone C-11) 100ng/mL[Final]

Figure 15

Subsequent to this initial screening result, column chromatography was employed to separate the unwanted byproduct and to afford progressively pure compound **X** (MW = 302). This was a very long and tedious process because the active compound and its

byproduct are very similar in polarity by TLC. **Figure 16** shows the gel performed on a more purified version of compound **X.** It is seen from **Figure 16** that the compound was 100% active at 20 µM concentration.

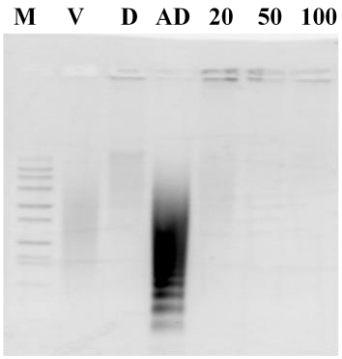

6.4x 10^6 cells/ml of Jurkat cells
M- Marker
V-Vehicle: 10µL of DMSO & 10µL of Methanol
D- Drug: 25µL Q-VD-OPh
AD- 10µL of AD
20- 10µL of **X** & 10µL of AD
50- 25µL of **X** & 10µL of AD
100- 50µL of **X** & 10µL of AD

Figure 16

Several methods were used to purify compound **X**, including prep TLC, liquid chromatography and standard column chromatography. Finally, after several purification procedures, compound **X** was isolated and shown to be pure by GC/MS analysis and ^{1}H and ^{13}C NMR spectral analyses. **Figure 17** shows the gel performed on the purest form of compound **X**.

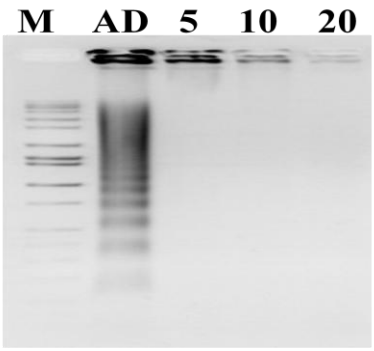

1.28 x 10^6 cells/ml of Jurkat cells
M- Marker
AD- Actinomyocin D only: 10µL of 1µg/µL Actinomyocin D + 10µL Methanol
5- 10µL of 5mM **X** + 10µl of 1µg/µL Actinomyocin D
10- 10µL of 10mM **X** + 10µl of 1µg/µL Actinomyocin D
20- 10µL of 20mM **X** + 10µl of 1µg/µL Actinomyocin D

Figure 17

Pure **X** was active at an astonishingly low concentration of 5 µM. This was a very promising result, since the commercially available Q-VD-OPh is also active at 5 µM.[5] It was also important to determine whether compound **X** was inhibiting apoptosis via caspases or not, and/or which caspase it was actually inhibiting. To do this, compound **X** was tested against other cysteine proteases. Cathepsins, which are cysteine proteases as well, are also responsible for carrying out apoptosis.[35] Cathepsins are synthesized in the lysosome of the cell as inactive enzymes called zymogens and are released when an intrinsic or extrinsic cell death signal is given.[35] The test against cathepsin L, which is the most common cathepsin secreted upon distress, was done by Dr. Scott Diamond and Dr. Tianhua from the University of Pennsylvania's Institute for Medicine and Engineering in Philadelphia, Pennsylvania. The testing was done on a blind basis, meaning that the personnel doing the testing did not know what the compounds were and that the compounds are tested twice for comparison purposes. The

compounds that were tested were compound **X** and compound **33**. For compound **X**, the result was an IC_{50} of 43µM against cathepsin L, which means that compound **X** is not a very active inhibitor of cathepsin L. Compound **33** tested negative.

Testing was also done against another class of cysteine proteases called calpains, which are also involved in signaling for apoptosis.[36,37] Calpains are activated when there is an increase in the Ca^{2+} ion concentration in the cytosol of the cell.[37] The calpain testing was done by Dr. Andrew Abell and Dr. Ondrej Zvarec from the School of Chemistry and Physics at The University of Adelaide in Adelaide, Australia. The testing was also done blindly and they too tested compounds **33** and **X.** The results from the calpain test show an IC_{50} of 3.3µM calpain inhibition for compound **X**, meaning that it is an average calpain inhibitor. The results from these two tests show that compound **X** is an average inhibitor of cathepsins and calpains. This is promising because for compound **X** to be caspase specific, it cannot be very active against other cysteine proteases. This would make it non-specific and therefore non-usable as a drug. The experiment that has yet to be done is to test compound **X** against the different caspases to see which one it is actually inhibiting and by which pathway.

Now that the inhibition activity was shown to be very effective, it was necessary to determine the actual structure of the inhibitor **X**. There were two possible areas that the nitro group would be expected to attack, the C-3 benzylidene ring or the aromatic portion of the heterocyclic oxindole ring. To determine the carbon most likely to be attacked by the electrophilic nitronium ion, ChemDraw Ultra was used to predict the ^{13}C

NMR shifts of the starting material **33.** **Figure 18** shows the ChemDraw predictions of the ^{13}C NMR shifts of **33**.

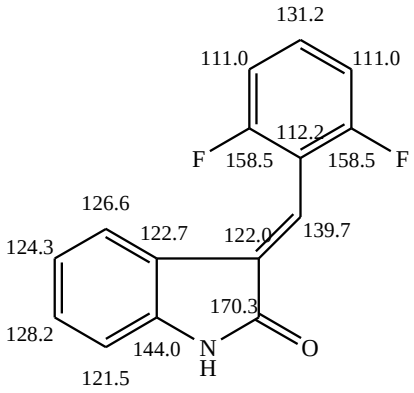

Figure 18

The carbon with the lowest value (ppm) will be the most likely place of nitration, being the most electron rich site on the compound. From **Figure 18**, the carbon with the highest electron density would be *ortho* to the fluorines on the C-3 benzylidene ring. This makes sense because fluorines are electronegative and will pull electron density away from the adjacent carbons and towards themselves by inductive effects, but are reasonably strong electron donors via resonance. With that in mind, an alternate synthesis was planned. The original procedure from **Scheme 19** was a very tedious procedure and an unwanted byproduct was formed every time the synthesis was performed. **Scheme 20** and **Scheme 21** show the new synthetic path expected to form compound **X**. Thus, 2,6-difluorobenzaldehyde (**41**) was nitrated using a literature procedure as shown in **Scheme 20**.[38] The product **42** was then condensed to **10** by an aldol condensation to afford **43** as shown in **Scheme 21**.

Scheme 20

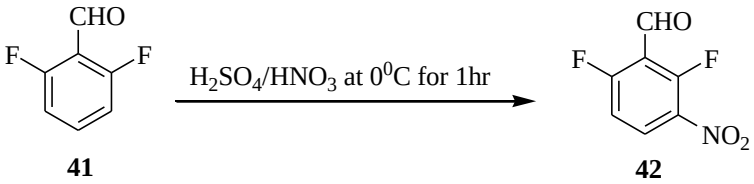

41 **42**

Scheme 21

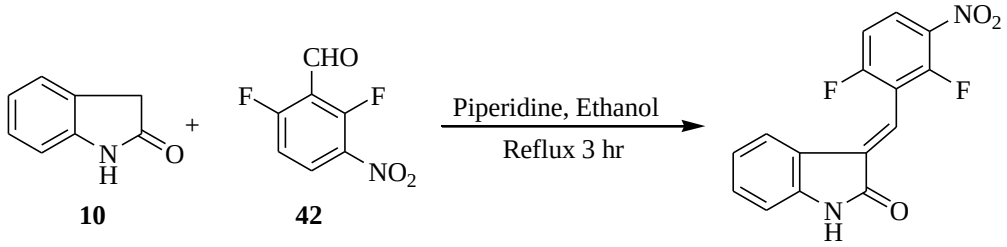

10 **42** **43**

Compound **42** was synthesized with relative ease and a yield of 17%. The reaction from **Scheme 21** gave product **43** with a yield of 12%. Product **43** was pure by TLC and GC/MS analysis did not show any signs of the 282 *m/z* byproduct that had been formed in the previous synthesis. The structure of compound **43** was confirmed by GC/MS and ^{13}C NMR spectroscopic analyses. The ^{13}C NMR spectrum for compound **43** is shown in **Figure 19**.

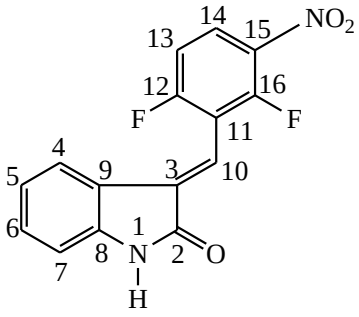

43

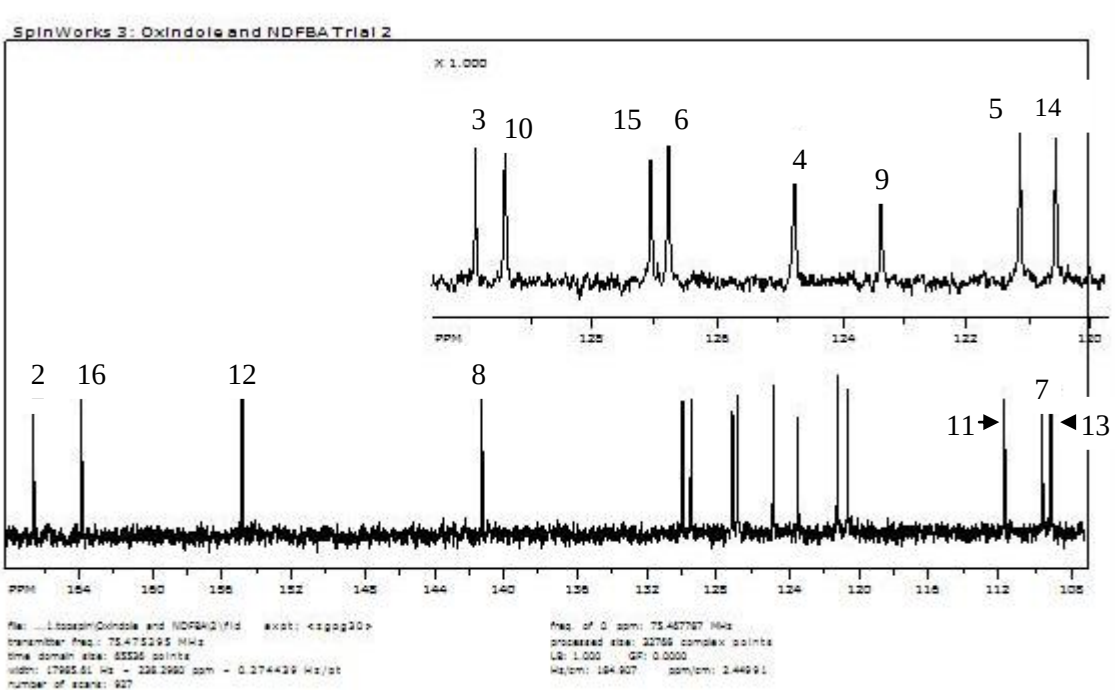

Figure 19

The ^{13}C NMR spectrum of **43** is different from the ^{13}C NMR of compound **X,** which raised some concern as to whether this compound was in fact the active compound **X**. In **Figure 19**, there are 15 signals that correspond to all of the signals in the structure of compound **43**. All of the signals in **Figure 19** are singlet peaks, while in the spectrum of compound **X** (not shown), the signals are experiencing different splitting patterns into doublets and triplets. There is also a difference in the number of signals between the two compounds **43** and **X**, which is a definitive indicator that the compounds are not the same. To determine whether compound **43** is active or not, a sample of it was sent to Dr. Brown for biological screening. The gel for compound **43** is shown in **Figure 20**. The compound had tested negative, even at 100 µM.

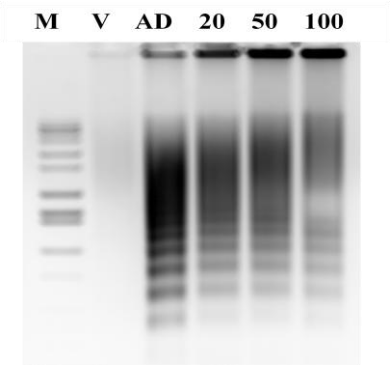

7.0 x 10^6 cells/ml of Jurkat cells
M- Marker
V-Vehicle: 20µL DMSO & 10µL CH_3OH
AD- Actinomycin D: 10µL AD
20- 4µL of **43** & 10µL AD
50- 10µL of **43** & 10µL AD
100- 20µL of **43** & 10µL AD

Figure 20

At this point, a pressing question arose as to what might be the actual structure of active compound **X**? Obviously the ChemDraw prediction of relative electron density of compound **33** (**Figure 18**) which indicated the most likely site of nitration was *ortho* to the fluorines was not correct otherwise compound **43** would have been active. It was then decided to take a closer look at the ^{13}C NMR spectra of the precursor **10** of the active compound **X**. An examination of the spectra of **10** (**Figure 13**), indicates that the carbon with the highest electron density is C-7, which has a signal at 109.99 ppm; a value which is consistent with the literature assignment.[34] Moreover, after a reaction with 2,6-difluorobenzaldehyde to form compound **33**, C-7 is still the most electron rich carbon with its signal at 110.12 ppm as shown in **Figure 14**. For comparison, the carbons adjacent to the fluorines, C-12 and C-12'are a doublet peak centered at ~112 ppm indicating that C-7 is the most electron rich carbon in compound **33**. Based on this interpretation of the ^{13}C NMR spectrum, the point of nitration on compound **33** would

most likely be C-7 and not C-12 or C-12'. To prove or disprove this theory, it was necessary to either prepare or purchase 7-nitrooxindole (**45**) and conduct its reaction with **33**. Purchasing **45** was economically prohibitive, since it is a custom synthetic compound. Examination of the literature revealed a procedure to synthesize **45** from 8-nitroquinoline (**44**).[39,40,41] The procedure involves using 30% H_2O_2 and acetic acid to oxidize **44** to form **45** through a proposed lactone intermediate.[42] This reaction procedure is shown in **Scheme 22**.

Scheme 22

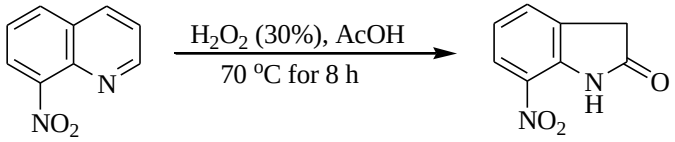

44 **45**

This reaction was performed under moderate conditions with relative ease. The yield of compound **45** was 14%, which was comparable to the literature yield of 20%.[42] Using **45** as the starting material, an aldol condensation was performed using **41** to form **46**. This procedure is shown in **Scheme 23**.

Scheme 23

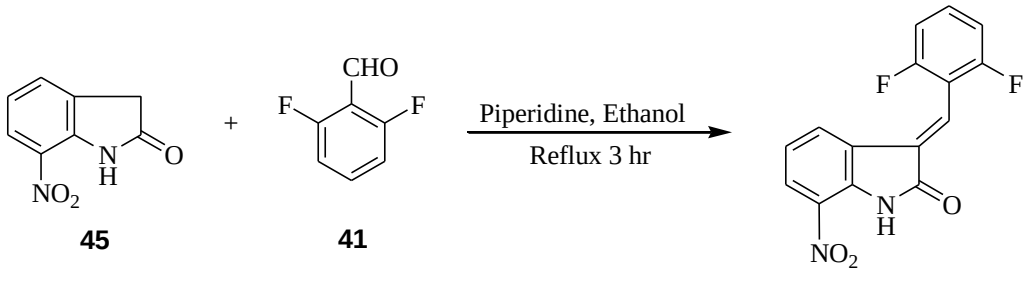

45 **41** **46**

Reviewing again, compound **46** was synthesized due to its likelihood of being the actual active compound **X** based on a consideration of the electron density at C-7 based

on ^{13}C NMR shifts. Unfortunately the results of the biological activity were not available by the time of the thesis defense.

While the initial goal of this project was to employ some of the structural features of Q-VD-OPh, the difficulties presented by the use of the 2,6-difluorophenyl substituent in terms of the defluorinated byproduct led us to examine a number of other possible aryl aldehydes in search of activity. In this regard, it is interesting to note that a 4-methoxy group on the aryl ring at the C-3 position demonstrated a low level of activity. This is noteworthy since our working hypothesis entailed nucleophilic attack by the cysteine residue of caspases on the β-carbon of the benzylidene oxindoles and a *para*-methoxy would be expected to reduce the electrophilicity of this position. Thus, the marginal activity of compound **32** (~50μM) came as somewhat of a surprise. The gel for active compound **32** is shown in **Figure 21**. The fact that this compound demonstrates may thus be an example of the non-electrophilic type of warhead suggested by Löser *et al*.[12]

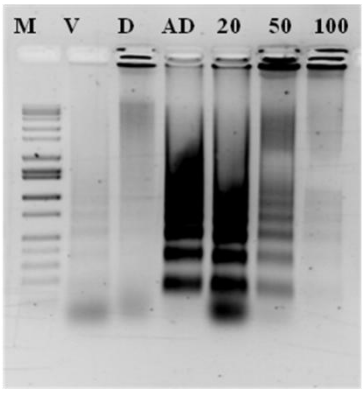

4 x 10^6 cells/ml of Jurkat cells
M- Marker
V-Vehicle: 20µL DMSO & 10µL Methanol
D- Drug: 20 µL of **32**
AD- 10 µL AD
20- 4µL of **32** & 10µL AD
50- 10µL of **32** & 10µL AD
100- 20µL of **32** & 10µL AD

Figure 21

The ^{13}C NMR spectrum of compound **32** is shown in **Figure 22.**

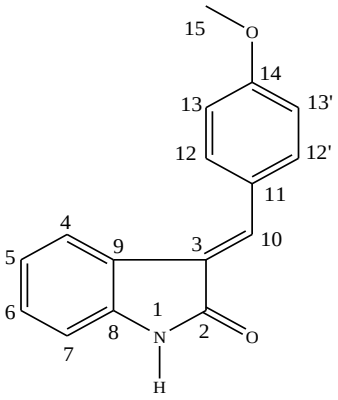

32

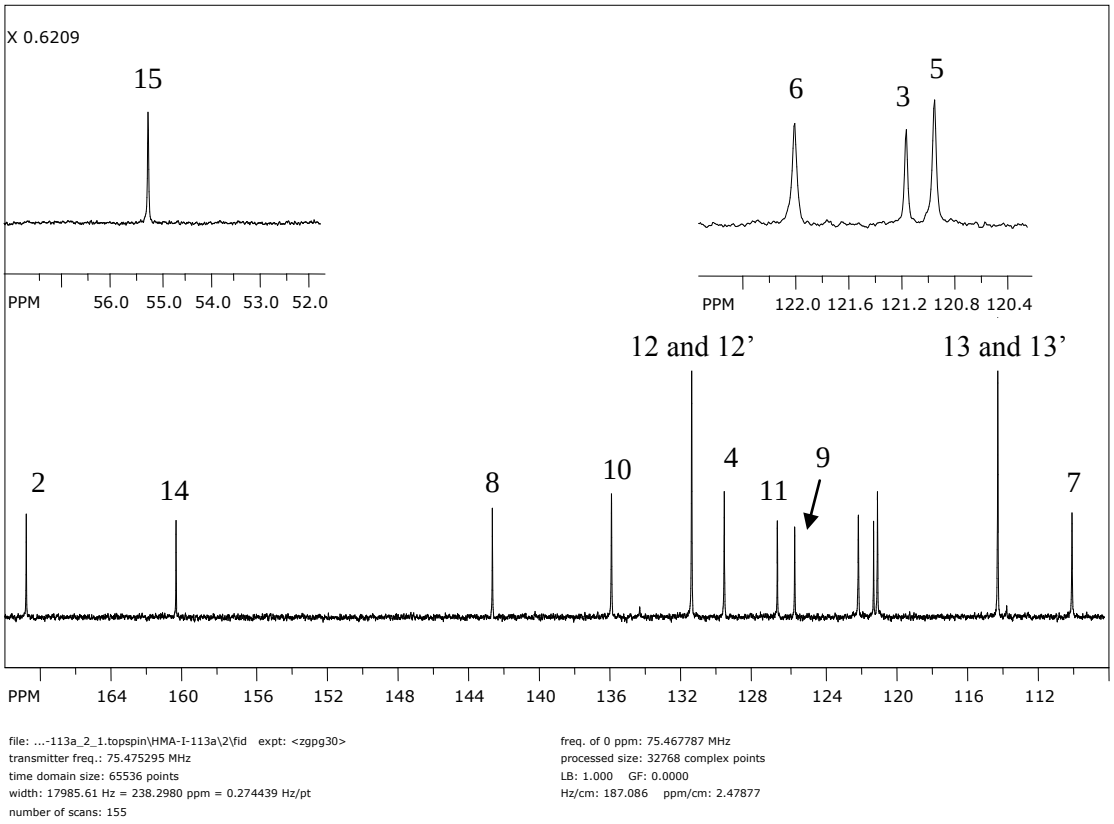

Figure 22

The product **32** was confirmed by ^{1}H and ^{13}C NMR spectroscopic analysis. **Figure 22** shows 14 signals in the ^{13}C NMR NMR that correspond to the structure for active compound **32**. The solvent used for this spectrum was DMSO-d_6, which appears at ~39.5 ppm. As can be seen, there is a peak in the aliphatic region at 55.26 ppm, which corresponds to the CH_3 of the methoxy group on C-15 while the C-2 amide carbonyl appears at 168.93 ppm. Also, the aromatic carbon bearing the methoxy group appears downfield with a signal at 160.48 ppm. Further examination of the other peaks in the aromatic region utilized ^{13}C DEPT 90 NMR to distinguish between the CH aromatic carbons and the quaternary aromatic carbons. The signal at 142.65 ppm appears in the

^{13}C NMR spectrum but not in the ^{13}C DEPT 90, meaning that it corresponds to the quaternary carbon labeled C-8. The signal at 135.94 ppm is present in both spectra, meaning that it is an aromatic CH carbon that corresponds to C-10. There are two intense signals that are also present in both spectra. They appear at 131.42 ppm and 114.17 ppm. The first signal can be identified as C-12 and C-12' as they are symmetrical CH carbons and the second signal is identified as C-13 and C-13' as they too are symmetrical carbons.

The original CH carbons on **10** do not shift very much from their original positions: C-4 at 122.02 ppm, C-5 at 120.95 ppm, C-6 at 129.58 ppm and C-7 at 109.98 ppm. The remaining quaternary aromatic carbons have lower intensity signals and are not visible in the ^{13}C DEPT 90 NMR. These are carbons C-3, C-9 and C-11. Carbon C-3 has a signal at 121.17 ppm, which is a dramatic shift downfield from the original oxindole (**10**) C-3 carbon. Carbon C-9 does not shift very much from its original position in **10**, with its signal at 125.61 ppm. The C-11 carbon signal is very close to C-9 with its signal showing at 126.59 ppm.

Finally, the third active compound might in some way be considered as mimicking the structural features of Q-VD-OPh in that it incorporates a pyridine ring which resembles the quinoline ring of the peptide inhibitor. Compound **31**, which has a nitrogen atom with an available lone pair of electrons at the C-4' position was found active at ~20 μM concentration. Hydrogen bonding between **31** and the active site on the caspase could be the mechanism of action of this non-electrophilic inhibitor. The gel for compound **31** is shown in **Figure 23**.

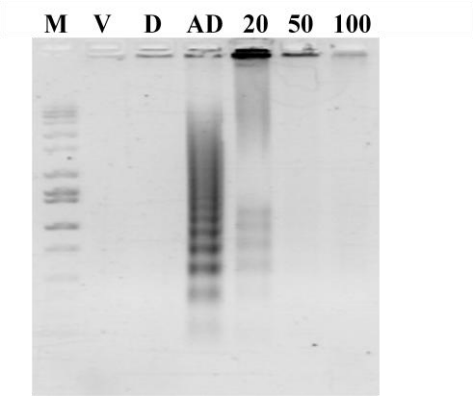

4.4 x 10^6 cells/ml of Jurkat cells
M- Marker
V-Vehicle: 20µL DMSO & 10µL CH_3OH
D- 20µL of **31**
AD- Actinomycin D: 10 µL AD
20- 4µL of **31** & 10µL AD
50- 10µL of **31** & 10µL AD
100- 20µL of **31** & 10µL AD

Figure 23

The structure for compound **31** could not be determined definitively by ^{13}C NMR spectroscopy due to it being a mixture of the *E* and *Z* configurations. The major isomer was determined by the melting point and its proximity to either of the two isomer's literature melting points.[29] Both the ^{13}C and ^{1}H NMR spectra have double the amount of signals expected for compound **31.**

FUTURE WORK

There is still a lot of work to be done to be able to say that an active and effective caspase inhibitor has been synthesized. More derivatives of the active compounds **X**, **31** and **32** need to be made to optimize the groups at the different positions and maximize inhibition capabilities. Hopefully compound **X**, once it is fully characterized and the synthesis is solid and repeatable with good yields, can be taken even further than just *in vitro* testing. I would like to see it tested on small animals and from there, go into clinical trials if it is safe and effective. As of now, I believe that my work has led to new ideas and new leads to pursue further. Beginning a project that no one has done before and achieving three active compounds in two years I believe is an accomplishment.

I would also like to see these active compounds tested against other apoptotic mechanisms. In this work, the testing was done against Human Jurkat T cells (Type 2 cells) by Dr. Thomas L. Brown. Testing these compounds against other apoptotic cells that may not be as common or as well known, such as retinal cells (in the eye) would be interesting to study. Retinal cell death is an area where small molecule apoptotic inhibitors have not been studied before, so it would broaden the scope of the use of these small molecule inhibitors as well.

EXPERIMENTAL

Chemical Analysis

Melting points were determined via the use of open capillaries with an Electrothermal melting point apparatus and are reported uncorrected. Elemental analyses were performed by Midwest Microlab, Indianapolis, IN. Elemental analysis results are within +0.4% of the theoretical values. The ^{1}H and ^{13}C NMR data were obtained on a Bruker Avance 300 MHz NMR in $CDCl_3$ solution unless otherwise indicated. The chemical shifts are reported in δ (ppm) downfield from tetramethylsilane as an internal standard; coupling constants (*J*) are in Hz. The following abbreviations are used to describe peak patterns where appropriate: s, singlet; d, doublet, dd, double doublet; t, triplet; q, quartet; dt, double triplet; m, multiplet. GC/MS measurements were performed using Hewlett-Packard 6890 Series GC with auto injection and mass fragments are reported as mass per charge, *m/z*. The GC was coupled with a mass spectrometer with a Hewlett-Packard 5973 mass selective detector/quadrupole system. Flash column (Silica Gel, Premium Rf, 200-400 mesh, Sorbent Technologies) and thin layer chromatography (TLC) were performed on silica gel with indicated solvent systems. All glassware and syringes were oven-dried for the reactions which require anhydrous conditions. The multimode microwave used for solventless reactions on silica gel was a GE JES638WF 700 Watt domestic microwave with a turn table with time and power controls. All microwave reactions were performed in a monomode Biotage Emery's Creator 300 Watt system and the MARS Glasschem 300 Watt system by CEM. It should be noted that all reactions

were run with sample absorption set to "normal". Multiple reactions were carried out using the FIRSTMATE system by Argonaut Technologies.

Biological Analysis

Human Jurkat T cells were treated with vehicle (V) or 1 mg/ml actinomycin D for four hours. DNA was isolated, and analyzed on a 1.2% agarose gel stained with ethidium bromide to determine DNA laddering. The agarose gel showed 50% functionality at 100 mm, resulting well below the inhibitory effects at 200 mm. Cytoplasmic DNA is small (less than 1500 bp) and is generated in apoptotic cells and can cross the nuclear membrane into the cytosol. If concentrations of the DNA are less than 200 mm, then cell inhibition is not justified.

5-Nitroindolin-2-one (12)

To a 25-mL Erlenmeyer flask in an ice bath containing sulfuric acid (1.9231 mL) and **10** (0.5121 g, 0.0038 mol) was added nitric acid (0.1615 mL) drop-wise with stirring. The mixture was stirred for 30 min after which the mixture was poured over ice. A brown colored solid (0.6030 g) was collected via vacuum filtration. Recrystallization using 50% acetic acid: water gave the pure product (beige color) (0.5621 g, 82%); mp 244-245 ^{o}C (lit. mp 240-241 ^{o}C)[13]; R_f = 0.55 (EtOAc); ^{1}H NMR (300 MHz, DMSO-d_6) δ 11.05 (s, 1H) 8.15 (d, J = 8.6 Hz, 1H), 8.09 (s, 1H), 6.97 (d, J = 8.6 Hz, 1H), 3.63 (s, 2H); ^{13}C NMR δ: 176.65, 150.24, 141.69, 127.00, 124.86, 119.95, 108.92, 35.56 ppm.

5-Nitroindoline-2,3-dione (13)

A solution of **7** (0.5 g, 3.4 mmol) in concentrated sulfuric acid (3.2 mL) was added dropwise to a solution of potassium nitrate (0.344 g, 3.4 mmol) in concentrated sulfuric acid (3.8 mL) in a 25-mL Erlenmeyer flask over a period of 1 h in an ice bath. The reaction mixture was poured over ice. The yellow-orange solid was collected via vacuum filtration (0.441 g, 67.5%). mp = 249-252°C (lit mp = 252-254 °C)[14]; R_f = 0.71 (EtOAc); ^{1}H NMR (300 MHz, DMSO-d_6) δ 11.67 (s, 1H), 8.45 (d, *J* = 8.71 Hz, 1H), 8.22 (s, 1H), 7.10 (d, *J* = 8.72 Hz, 1H)

1-(2,6-Difluorobenzyl)indoline-2,3-dione (17)

In a vial with acetonitrile (3 mL) was dissolved isatin (0.3 g, 0.00204 mol) and KF/Alumina (1 equiv, 0.1185 g, 0.00204 mol). 2,6-Difluorobenzyl bromide (2 equiv, 0.8446 g, 0.00408 mol) was added to the vial. The vial was placed on a 30 °C hot plate for 5 days. The vial was then heated at 50 °C for 48 h. Deionized water was added to the vial and stirred for 6 days at room temperature. Bright orange solid was collected via vacuum filtration (0.2066 g, 37.1 %). mp = 178-185 ^{o}C; R_f = 0.89 (EtOAc); ^{1}H NMR (300 MHz, DMSO-d_6) δ 7.60 (d, *J* = 6.60 Hz, 1H), 7.53 (dt, *J* = 7.82 Hz, 1H), 7.36-7.27 (m, 1H), 7.31 (t, *J* = 6.55 Hz), 7.10 (t, *J* = 7.35 Hz, 1H), 6.94 (t, *J* = 8.20 Hz, 1H), 5.03, (s, 1H).

Attempted Synthesis of (18)

In a vial with acetonitrile (3 mL) was dissolved **7** (0.3 g, 0.00204 mol) and KF/Alumina (1 equiv, 0.1185 g, 0.00204 mol). Ethyl acrylate (2 equiv, 0.4085 g, 0.00408 mol) was added to the vial. The vial was placed on a 30°C hot plate for 5 days. The vial was then heated at 50 °C for 48 hrs. Deionized water was added to the vial and stirred for 6 days at room temperature. The product was an oily substance. The synthesis yielded only starting material based on the melting point.

Attempted Synthesis of (19)

In a vial with acetonitrile (3 mL) was dissolved **7** (0.3 g, 0.00204 mol) and KF/Alumina (1 equiv, 0.1185 g, 0.00204 mol). Ethyl bromoacetate (2 equiv, 0.6814 g, 0.00408 mol) was added to the vial. The vial was placed on a 30°C hot plate for 5 days. The vial was then heated at 50 °C for 48 hrs. Deionized water was added to the vial and stirred for 6 days at room temperature. The product was an oily substance (0.2168 g, 45.6 %). mp = 190-197 ^{o}C (lit mp = 132-133 °C)[23]; R_f = 0.83 (EtOAc). The synthesis yielded only starting material based on the melting point.

Attempted Synthesis of (20)

In a vial with acetonitrile (3 mL) was dissolved **7** (0.3 g, 0.00204 mol) and KF/Alumina (1 equiv, 0.1185 g, 0.00204 mol). Benzyl chloride (2 equiv, 0.5165 g, 0.00408 mol) was added to the vial. The vial was placed on a 30°C hot plate for 5 days. The vial was then heated at 50 °C for 48 hrs. Deionized water was added to the vial and stirred for 6 days at room temperature. The product (bright orange) was collected by vacuum filtration (0.2251 g, 46.5 %). mp = 196-199 ^{o}C (lit mp = 133-134 °C)[23]; R_f = 0.63 (EtOAc). The synthesis yielded only starting material based on the melting point.

***tert*-Butyl 3-(2,3-dioxoindolin-1-yl)propanoate (21)**

In a vial with acetonitrile (3 mL) was dissolved **7** (0.3 g, 0.00204 mol) and KF/Alumina (1 equiv, 0.1185 g, 0.00204 mol). *t*-Butyl acrylate (2 equiv, 0.5229 g, 0.00408 mol) was added to the vial. The vial was placed on a 30 °C hot plate for 5 days. The vial was then heated at 50 °C for 48 h. Deionized water was added to the vial and stirred for 6 days at room temperature. A silica gel column was performed using 70:30 Hexanes: EtOAc to afford an orange- red oil. (0.14 g, 24.9%) mp = N/A; R_f = 0.83 (EtOAc); ^{1}H NMR (300 MHz, DMSO-d_6) δ 7.68 (t, *J* = 15.6 Hz, 1H), 7.56 (d, *J* = 7.41 Hz, 1H), 7.25 (d, *J* = 7.96 Hz, 1H), 7.14 (t, *J* = 15.0 Hz, 1H), 3.89 (t, *J* = 14.1 Hz, 2H), 2.60 (t, *J* = 14.1 Hz, 2H), 1.35 (s, 3H).

Ethyl 2-(2,3-dioxoindolin-1-yl)acetate (22)

Compound **7** (2 g, 13.6 mmol) and CaH_2 (1 equiv, 0.5720 g, 13.6 mmol) were dissolved in DMF (6.61 g) in a vial and stirred at 100°C for 1 h. The solution was cooled to 40°C so that ethyl bromoacetate (3 equiv, 6.812 g, 40.8 mmol) could be added to the vial. The vial was placed back on the hot plate at 100°C for 4h then cooled to room temp. The solution was poured into an aqueous solution of 0.5 M HCl (40 mL) stirring vigorously. Orange precipitate was collected via vacuum filtration. Product was recrystallized using a 50% DCM/hexanes solution to afford a yellow product (1.2139 g, 38.3%). mp = 124-128°C (lit mp = 132-133 °C)[23]; R_f = 0.70 (EtOAc); ^{1}H NMR (300 MHz, DMSO-d_6) δ 7.69 (t, *J* = 15.5 Hz, 1H), 7.62 (d, *J* = 7.39 Hz, 1H), 7.19 (t, *J* = 16.6 Hz, 1H), 4.63 (s, 2H), 4.18 (q, *J* = 14.17 Hz, *J* = 7.07 Hz, 2H), 1.22 (t, *J* = 14.2 Hz, 3H)

1-Benzylindoline-2,3-dione (23)

Compound **7** (2 g, 13.6 mmol) and CaH_2 (1 equiv, 0.5720 g, 13.6 mmol) were dissolved in DMF (6.61 g) in a vial and stirred at 100°C for 1 h. The solution was cooled to 40°C so that benzyl chloride (3 equiv, 5.165 g, 40.8 mmol) could be added to the vial. The vial was placed back on the hot plate at 100°C for 4h then cooled to room temp. The solution was poured into an aqueous solution of 0.5 M HCl (40 mL) stirring vigorously. Red precipitate was collected via vacuum filtration. Product was recrystallized using a 50% DCM/hexanes solution to afford an orange product (0.486 g, 15.1%). mp = 134-139°C (lit mp = 133-134 °C)[23]; R_f = 0.86 (EtOAc); ^{1}H NMR (300 MHz, DMSO-d_6) δ 7.66 (d, *J* = 7.31 Hz, 1H), 7.57 (d, *J* = 6.65 Hz, 1H), 7.21 (t, *J* = 14.1 Hz, 1H), 6.98 (d, *J* = 8.18 Hz, 1H), 6.72 (t, *J* = 17.9 Hz, 1H), 6.57 (t, *J* = 14.7 Hz, 1H), 6.50 (t, *J* = 14.9 Hz, 1H), 4.91 (s, 2H).

(*Z*)-3-((1H-pyrrol-2-yl)methylene)-5-nitroindolin-2-one (24)

In a FIRSTMATE reaction tube with a stir bar was combined **12** (0.3385 g, 0.0019 mol) with pyrrole-2-carboxaldehyde (1.2 equiv, 0.2161 g, 0.00228 mol) and piperidine (0.10 equiv, 0.0194 g, 0.000228 mol) and EtOH (2 mL). The reaction tube was placed in the holder and the system was set to the following parameters: interval = 5, up stroke = 4, speed = max, hot plate temp = 90 °C, time = 3 h and inert gas = Argon. Reddish-brown solid (0.4658 g, 96.1%) was collected via vacuum filtration: mp = >295 °C (lit mp = 308-310 °C)[32]; R_f = 0.77 (EtOAc); ^{1}H NMR (300 MHz, DMSO-d_6) δ 11.49 (s, 1H), 8.53 (d, *J* = 2.17 Hz, 1H), 8.09 (s, 1H, H_{vinyl}), 8.04 (dd, *J* = 8.61 and 2.23 Hz, 1H), 7.44 (s, 1H), 7.01 (d, *J* = 8.61 Hz, 1H), 6.41 (dd, *J* = 5.8 and 2.24 Hz, 1H).

(*E*)-3-(2-chlorobenzylidene)-5-nitroindolin-2-one (25)

In a FIRSTMATE reaction tube with a stir bar was combined **12** (0.3385 g, 0.0019 mol) with 2-chlorobenzaldehyde (1.2 equiv, 0.3258 g, 0.00228 mol) and piperidine (0.10 equiv, 0.0194 g, 0.000228 mol) and EtOH (2 mL). The reaction tube was placed in the holder and the system was set to the following parameters: interval = 5, up stroke = 4, speed = max, hot plate temp = 90 °C, time = 3 h and inert gas = Argon. Green-yellow solid (0.1148 g, 20.1%) was collected via vacuum filtration: mp = 269-271 °C; R_f = 0.74 (EtOAc); Compound **25** would not dissolve in any of the deuterated NMR solvents, therefore an NMR spectrum could not be generated.

(*E*)-3-(2-(trifluoromethyl)benzylidene)-5-nitroindolin-2-one (26)

In a FIRSTMATE reaction tube with a stir bar was combined **12** (0.3385 g, 0.0019 mol) with trifluoro-*o*-tolualdehyde (1.2 equiv, 0.4151 g, 0.00228 mol) and piperidine (0.10 equiv, 0.0194 g, 0.000228 mol) and EtOH (2 mL). The reaction tube was placed in the holder and the system was set to the following parameters: interval = 5, up stroke = 4, speed = max, hot plate temp = 90 °C, time = 3 h and inert gas = Argon. Yellow solid (0.2922 g, 46.0%) was collected via vacuum filtration: mp = 218-221 °C; R_f = 0.75 (EtOAc); ^{1}H NMR (300 MHz, DMSO-d_6) δ 11.46 (s, 1H), 7.97 (d, *J* = 7.59 Hz, 1H), 7.90 (s, 1H), 7.86 (s, 3H), 7.83-7.78 (m, 1H), 7.60 (s, 1H, H_{vinyl}), 7.06 (d, *J* = 8.69 Hz, 1H, C-6').

(*Z*)-3-(3-methylbutylidene)-5-nitroindolin-2-one (27)

In a FIRSTMATE reaction tube with a stir bar was combined **12** (0.3385 g, 0.0019 mol) with isovaleraldehyde (1.2 equiv, 0.2205 g, 0.00228 mol) and piperidine (0.10 equiv, 0.0194 g, 0.000228 mol) and EtOH (2 mL). The reaction tube was placed in the holder and the system was set to the following parameters: interval = 5, up stroke = 4, speed = max, hot plate temp = 90 °C, time = 3 h and inert gas = Argon. Off-white solid (0.2894 g, 61.9%) was collected via vacuum filtration: mp = 231-234 °C; R_f = 0.68 (EtOAc); ^{1}H NMR (300 MHz, DMSO-d_6) δ 10.80 (s, 1H), 7.77 (s, 1H, H_{vinyl}), 6.86 (d, *J* = 8.66 Hz, 1H), 6.60 (d, *J* = 11.18 Hz, 1H), 6.40 (d, *J* = 7.46 Hz, 2H), 3.70 (d, *J* = 11.73 Hz, 2H), 1.85-1.53 (m, 1H), 1.18 (s, 3H).

(*E*)-3-(2,6-difluorobenzylidene)-5-nitroindolin-2-one (28)

In a vial was combined **12** (0.4023 g, 0.0022 mol) with 2,6-difluorobenzaldehyde (1.2 equiv, 0.3837 g, 0.0027 mol) and piperidine (0.10 equiv, 26.7µL, 0.00027 mol) and EtOH (4 mL) with stirring. The vial was placed on a 90 °C hot plate for 3 h. Product was recrystallized using acetic acid to afford a yellow solid (0.6062 g, 89%) collected via vacuum filtration; mp = 251-255 °C; R_f = 0.78 (EtOAc); ^{1}H NMR (300 MHz, DMSO-d_6) δ 11.45 (s, 1H), 8.75 (s,1H), 8.21 (d, *J* = 8.7 Hz, 1H), 7.75-7.66 (m, 1H), 7.57 (s, 1H, H_{vinyl}), 7.36 (t, *J* = 8.34 Hz, 1H), 7.16 (t, *J* = 7.99 Hz, 1H), 7.07 (d, *J* = 8.69 Hz, 1H); ^{13}C NMR δ: 167.77, 161.27-157.86 (dd, *J* = 7.24 Hz), 148.86, 141.87, 133.03 (t, *J* = 10.51 Hz), 130.16, 127.20, 123.31, 120.89, 118.30, 112.48- 112.46 (dd, *J* = 6.41 Hz), 111.44-111.20 (t, *J* = 8.71 Hz), 110.27 ppm.

(*E*)-3-(3,5-difluorobenzylidene)-5-nitroindolin-2-one (29)

In a vial was combined **12** (0.1238 g, 0.00067 mol) with 3,5-difluorobenzaldehyde (1.2 equiv, 0.1150 g, 0.00081 mol) and piperidine (0.10 equiv, 0.069 g, 0.000081 mol, 10.4 µL) and EtOH (1 mL) with stirring. The vial was placed on a 90 °C hot plate for 3 hrs. Golden solid (0.1075 g, 53.1%) was collected via vacuum filtration: mp = 301-306 °C; R_f = 0.72 (EtOAc); ^{1}H NMR (300 MHz, DMSO-d_6) δ 11.37 (s, 1H), 8.53 (s, 1H), 8.14-8.02 (m, 1H), 7.71 (s, 1H, H_{vinyl}), 7.02 (d, *J* = 8.72 Hz, 1H, C-2'), 6.96 (d, *J* = 8.53 Hz, 1H), 2.51 (s, 1H).

(*E*)-3-(4-hydroxybenzylidene)-indolin-2-one (30)

In a vial was combined **10** (0.2500 g, 0.0019 mol) with 4-hydroxybenzaldeyhde (1.2 equiv, 0.2860 g, 0.0023 mol) and piperidine (0.10 equiv, 0.00023 mol, 23 μL) and EtOH (2 mL) with stirring. The vial was placed on a 90 °C hot plate for 3 h. A yellow solid (0.2706 g, 60%) was collected via vacuum filtration: mp = 298-301 °C (lit mp = 300+ °C)[28]; R_f = 0.43 (50:50 Hexanes:EtOAc); ^{1}H NMR (300 MHz, DMSO-d_6) δ 10.91 (s, 1H), 8.10 (d, *J* = 7.67 Hz, 1H), 8.03 (d, *J* = 8.47 Hz, 1H), 7.96 (s, 1H), 7.61 (d, *J* = 7.63 Hz, 1H, C-2'), 7.31 (d, *J* = 13.78 Hz, 1H), 7.31 (s, 1H, H_{vinyl}), 7.27 (d, *J* = 4.69 Hz, 1H); ^{13}C NMR δ: 169.46, 159.67, 142.86, 132.17, 129.77, 125.41, 125.07, 122.41, 121.70, 121.38, 116.31, 110.32 ppm.

(*Z*)-3-((pyridin-4-yl)methylene)indolin-2-one (31)

In a vial was combined **10** (0.2508 g, 0.0019 mol) with 4-pyridinecarboxaldehyde (1.2 equiv, 217 μL, 0.0023 mol) and piperidine (0.10 equiv, 0.00023 mol, 23 μL) and EtOH (2 mL) with stirring. The vial was placed on a 90 °C hot plate for 3 h. A yellow solid (0.2524 g, 60%) was collected via vacuum filtration: mp = 226-229 °C (lit mp = 225-226 °C)[29]; R_f = 0.12 (50:50 Hexanes:EtOAc); Compound **31** was a mixture of *E* and *Z* isomers, therefore an NMR spectrum could not be determined.

(*E*)-3-(4-methoxybenzylidene)indolin-2-one (32)

In a vial was combined **10** (0.2532 g, 0.0019 mol) with *p*-anisaldehyde (1.2 equiv, 280 μL, 0.0023 mol) and piperidine (0.10 equiv, 0.00023 mol, 23 μL) and EtOH (2 mL) with stirring. The vial was placed on a 90 °C hot plate for 3 h. A yellow solid (0.1463 g, 31%) was collected via vacuum filtration: mp = 152-155 °C (lit mp = 156-157 °C)[18,30]; R_f = 0.17 (50:50 Hexanes:EtOAc); ^{1}H NMR (300 MHz, DMSO-d_6) δ 10.56 (s, 1H), 7.67 (t, *J* = 8.92 Hz, 1H), 7.59 (s,1H, H_{vinyl}), 7.20 (t, *J* = 7.51 Hz, 1H), 7.06 (d, *J*= 8.07 Hz, 1H, C-2'), 6.87 (t, *J* = 5.99 Hz, 1H), 6.83 (s, 1H), 2.50 (s, 3H); ^{13}C NMR δ: 168.93, 160.48, 142.65, 135.94, 131.42, 129.59, 126.59, 125.61, 122.02, 121.16, 120.95, 114.17, 109.98, 55.26 ppm.

(*E*)-3-(2,6-difluorobenzylidene)indolin-2-one (33) (Procedure 1)

In a vial was combined **10** (0.25 g, 0.0019 mol) with 2,6-difluorobenzaldehyde (1.1 equiv, 0.2984 g, 0.0021 mol) and piperidine (10 equiv, 1.7882 g, 0.021 mol) and EtOH (2 mL). The vial was placed on a 70°C hot plate for 48 h. Yellow solid (0.1032 g, 21.1%) was collected via vacuum filtration. mp = 220-223°C; R_f = 0.65 (EtOAc); ^{1}H NMR (300 MHz, DMSO-d_6) δ 10.73 (s, 1H), 7.67-7.57 (m, 1H), 7.34 (d, *J* = 14.5 Hz, 1H), 7.30 (d, *J* = 16.4, 1H), 7.24 (s, 1H, H_{vinyl}), 6.89 (dd, *J* = 15.3 and 7.5 Hz, 1H); ^{13}C NMR δ: 167.53, 161.32-157.92 (dd, *J* = 7.02 Hz), 143.23, 132.29, 131.93 (t, *J* = 10.44 Hz), 130.80, 123.09, 121.46, 120.70, 119.71, 112.25- 111.75 (d, *J* = 24.64 Hz), 112.16-111.75 (t, *J* = 19.74 Hz), 110.12 ppm.

(*E*)-3-(2,6-difluorobenzylidene)indolin-2-one (33) (Procedure 2)

In a vial was combined **10** (0.25 g, 0.0019 mol) with 2,6-difluorobenzaldehyde (1.2 equiv, 0.3240 g, 0.00228 mol) and piperidine (0.10 equiv, 0.0194 g, 0.000228 mol) and EtOH (2 mL) with stirring. The vial was placed on a 90 °C hot plate for 3 h. Yellow solid (0.3929 g, 79%) was collected via vacuum filtration. mp = 210-215 °C; R_f = 0.69 (EtOAc); ^{1}H NMR (300 MHz, $CDCl_3$-d_1) δ 8.27 (s, 1H), 7.47-7.37 (m, 1H), 7.26 (s, 1H, H_{vinyl}), 7.23 (d, *J* = 8.16 Hz, 1H), 7.05 (dd, *J* = 15.3 and 7.5 Hz, 1H), 6.89 (d, *J* = 7.84 Hz, 1H); ^{13}C NMR δ: 167.53, 161.32-157.92 (dd, *J* = 7.02 Hz), 143.23, 132.29, 131.93 (t, *J* = 10.44 Hz), 130.80, 123.09, 121.46, 120.70, 119.71, 112.25- 111.75 (d, *J* = 24.64 Hz), 112.16- 111.75 (t, *J* = 19.74 Hz), 110.12 ppm.

(*E*)-3-(2,6-difluorobenzylidene)indolin-2-one (33) (Microwave Synthesis)

To a Glasschem 20 vessel with a stir bar was added **10** (0.5 g, 0.0038 mol) with 2,6-difluorobenzaldehyde (1.2 equiv, 0.6480 g, 0.00456 mol) and piperidine (0.10 equiv, 0.0388 g, 0.000456 mol) and EtOH (4 mL). The power on the MARS Glasschem Microwave was set to 300W, ramp to temp time = 2:00 min., hold temp = 5:00 min., set temp = 140°C and stir bar speed = 3 (high). These parameters were collectively saved as method name "Hagar". Yellow solid (0.5369 g, 55.3%) was collected via vacuum filtration. mp = 213-218 °C; R_f = 0.85 (EtOAc); ^{1}H NMR (300 MHz, DMSO-d_6) δ 10.72 (s, 1H), 7.68-7.58 (m, 1H), 7.34 (d, *J* = 3.7 Hz, 1H), 7.31 (s, 1H, H_{vinyl}), 7.25 (d, *J* = 2.08 Hz, 1H), 6.89 (dd, *J* = 14.4 and 7.1 Hz, 1H); ^{13}C NMR δ: 167.53, 161.32-157.92 (dd, *J* = 7.02 Hz), 143.23, 132.29, 131.93 (t, *J* = 10.44 Hz), 130.80, 123.09, 121.46, 120.70, 119.71, 112.25- 111.75 (d, *J* = 24.64 Hz), 112.16- 111.75 (t, *J* = 19.74 Hz), 110.12 ppm. Anal. Calcd for $C_{15}H_9NOF_2$: C, 70.04; H, 3.53; N, 5.45. Found: C, 69.90; H, 3.71; N, 5.62

(*E*)-3-(3,5-difluorobenzylidene)indolin-2-one (34)

In a vial was combined **10** (0.2998 g, 0.0023 mol) with 3,5-difluorobenzaldehyde (1.2 equiv, 0.4170 g, 0.0027 mol) and piperidine (0.10 equiv, 0.023 g, 0.00027 mol, 27 μL) and EtOH (2 mL) with stirring. The vial was placed on a 90 °C hot plate for 3 hrs. Golden solid (0.2819 g, 47.6%) was collected via vacuum filtration: mp = 202-205 °C; R_f = 0.79 (EtOAc); ^{1}H NMR (300 MHz, DMSO-d_6) δ 10.68 (s, 1H), 8.10 (d, *J* = 7.56 Hz, 1H), 7.72 (s, 1H, H_{vinyl}), 7.65 (d, *J* = 7.56 Hz, 1H, C-2'), 8.14-8.01 (m, 1H), 6.98 (dd, *J* = 20.12 Hz, 9.15 Hz, 1H); Anal. Calcd for $C_{15}H_9NOF_2$: C, 70.04; H, 3.53; N, 5.45. Found: C, 69.65; H, 3.69; N, 5.42.

***(E)*-3-(2,3-dichlorobenzylidene)indolin-2-one (35)**

In a vial was combined **10** (0.2497 g, 0.0019 mol) with 2,3-dichlorobenzaldehyde (1.2 equiv, 0.3945 g, 0.0023 mol) and piperidine (0.10 equiv, 0.00023 mol, 23 μL) and EtOH (2 mL) with stirring. The vial was placed on a 90 °C hot plate for 3 h. A yellow-orange solid (0.4807 g, 89%) was collected via vacuum filtration: mp = 263-265 °C; R_f = 0.68 (50:50 Hexanes:EtOAc); ^{1}H NMR (300 MHz, DMSO-d_6) δ 10.70 (s, 1H), 7.75 (d, *J* = 8.00 Hz, 1H), 7.72 (d, *J* = 7.64 Hz, 1H), 7.55 (s, 1H, H_{vinyl}), 7.51 (t, *J* = 7.93 Hz, 1H), 7.24 (t, *J* = 7.67 Hz, 1H), 7.07 (d, *J* = 7.64 Hz, 1H, C-6'), 6.88 (d, *J* = 7.78 Hz, 1H), 6.81 (t, *J* = 7.64 Hz, 1H)

(*E*)-3-benzylideneindolin-2-one (36)

In a vial was combined **10** (0.2515 g, 0.0019 mol) with benzaldehyde (1.2 equiv, 0.4283 g, 0.0023 mol) and piperidine (0.10 equiv, 0.00023 mol, 23 μL) and EtOH (2 mL) with stirring. The vial was placed on a 90 °C hot plate for 3 h. A yellow solid (0.3831 g, 62%) was collected via vacuum filtration: mp = 172-175 °C (lit mp = 175-176 °C)[30,31]; R_f = 0.41 (50:50 Hexanes:EtOAc); ^{1}H NMR (300 MHz, DMSO-d_6) δ 10.61 (s, 1H), 7.69 (d, *J* = 7.26 Hz, 1H), 7.64 (s, 1H, H_{vinyl}), 7.49 (t, *J* = 7.62 Hz, 1H), 7.22 (t, *J* = 7.67 Hz, 1H), 6.88 (d, *J* = 7.98 Hz, 1H, C-2'), 6.83 (t, *J* = 7.65 Hz, 1H).

(*Z*)-3-(4-nitrobenzylidene)indolin-2-one (37)

In a vial was combined **10** (0.2503 g, 0.0019 mol) with 4-nitrobenzaldehyde (1.2 equiv, 214 μL, 0.0023 mol) and piperidine (0.10 equiv, 0.00023 mol, 23 μL) and EtOH (2 mL) with stirring. The vial was placed on a 90 °C hot plate for 3 h. A yellow solid (0.2785 g, 68%) was collected via vacuum filtration: mp = 251-252 °C (lit mp = 252-253 °C)[30]; R_f = 0.41 (50:50 Hexanes:EtOAc); ^{1}H NMR (300 MHz, DMSO-d_6) δ 10.68 (s, 1H), 8.32 (d, *J* = 8.24 Hz, 1H, C-2'), 7.93 (d, *J* = 8.19 Hz, 1H), 7.65 (s, 1H, H_{vinyl}), 7.39 (d, *J* = 8.24 Hz, 1H), 7.49 (d, *J* = 7.48 Hz, 1H), 7.25 (t, *J* = 7.42 Hz, 1H), 6.86 (t, *J* = 8.31 Hz, 1H)

(*Z*)-3-(2-fluoro-5-nitrobenzylidene)indolin-2-one (38)

In a vial was combined **10** (0.2507 g, 0.0019 mol) with 2-fluoro-5-nitrobenzaldehyde (1.2 equiv, 0.3834 g, 0.0023 mol) and piperidine (0.10 equiv, 0.00023 mol, 23 μL) and EtOH (2 mL) with stirring. The vial was placed on a 90 °C hot plate for 3 h. A yellow solid (0.3472 g, 65%) was collected via vacuum filtration: mp = 199-201 °C; R_f = 0.59 (50:50 Hexanes:EtOAc); ^{1}H NMR (300 MHz, DMSO-d_6) δ 10.60 (s, 1H), 8.33 (s, 1H, C-6'), 8.02 (d, *J* = 7.65 Hz, 1H), 7.64 (d, *J* = 8.42 Hz, 1H), 7.40 (d, *J* = 8.24 Hz, 1H), 7.33 (s, 1H, H_{vinyl}), 7.25 (d, *J* = 7.61 Hz, 1H), 6.84 (t, *J* = 7.84 Hz, 1H).

(*E*)-3-(2-chloro-3,6-difluorobenzylidene)indolin-2-one (39)

In a vial was combined **10** (0.2497 g, 0.0019 mol) with 2-chloro-3,6-difluorobenzaldehyde (1.2 equiv, 0.3993 g, 0.0023 mol) and piperidine (0.10 equiv, 0.00023 mol, 23 μL) and EtOH (2 mL) with stirring. The vial was placed on a 90 °C hot plate for 3 h. A yellow solid (0.3472 g, 65%) was collected via vacuum filtration: mp = 199-201 °C; R_f = 0.59 (50:50 Hexanes:EtOAc); ^{1}H NMR (300 MHz, DMSO-d_6) δ 10.53 (s, 1H), 7.79 (d, *J* = 8.24 Hz, 1H), 7.54 (s, 1H, H_{vinyl}), 7.46 (d, *J* = 7.61 Hz, 1H), 7.22 (t, *J* = 8.01 Hz, 1H), 7.17 (t, *J* = 7.57 Hz, 1H), 7.08 (d, *J* = 7.76 Hz, 1H), 6.95 (d, *J* = 7.24 Hz, 1H)

(*E*)-3-(2,3,5-trichlorobenzylidene)indolin-2-one (40)

In a vial was combined **10** (0.2515 g, 0.0019 mol) with 2,3,5-trichlorobenzaldehyde (1.2 equiv, 0.4283 g, 0.0023 mol) and piperidine (0.10 equiv, 0.00023 mol, 23 μL) and EtOH (2 mL) with stirring. The vial was placed on a 90 °C hot plate for 3 h. An orange solid (0.3831 g, 62%) was collected via vacuum filtration: mp = 268-270 °C; R_f = 0.60 (50:50 Hexanes:EtOAc); Compound **40** would not dissolve in any of the deuterated NMR solvents, therefore an NMR spectrum could not be generated.

2,6-difluoro-3-nitrobenzaldehyde (42)

Sulfuric acid (11mL) was added to a beaker and cooled in an ice bath so that the temperature did not exceed 5 °C. 2,6-Difluorobenzaldehyde (2.4 mL, 0.0222 mol) was added to the beaker dropwise. Nitric acid (900 μL) was added to the beaker and the solution was left to stir for 1 h. The product (off-white) was collected by vacuum filtration (0.7104 g, 17%); mp = 59-61 °C; R_f = 0.62 (50:50 Hexanes:EtOAc); ^{1}H NMR (300 MHz, DMSO-d_6) δ 10.20 (s, 1H), 8.56-8.48 (m, 1H), 7.51 (t, J = 9.51 Hz, 1H).

(*E*)-3-(2,6-difluoro-3-nitrobenzylidene)indolin-2-one (43)

In a vial was combined **10** (0.2571 g, 0.0019 mol) with **42** (1.2 equiv, 0.4324 g, 0.0023 mol) and piperidine (0.10 equiv, 0.00023 mol, 23 μL) and EtOH (2 mL) with stirring. The vial was placed on a 90 °C hot plate for 3 h. A yellow solid (0.0705 g, 12%) was collected via vacuum filtration: mp = 220-225 °C; R_f = 0.46 (50:50 Hexanes:EtOAc); ^{1}H NMR (300 MHz, DMSO-d_6) δ 10.45 (s, 1H), 8.00 (d, *J* = 9.40 Hz, 1H), 7.70 (d, *J* = 7.49 Hz, 1H), 7.47 (s, 1H, H_{vinyl}), 7.23 (t, *J* = 7.66 Hz, 1H), 6.99 (t, *J* = 7.53 Hz, 1H), 6.83 (d, *J* = 7.74 Hz, 1H), 6.59 (d, *J* = 9.41 Hz, 1H).

7-Nitroindolin-2-one (45)

In a vial was combined 8-nitroquinoline (1.9998 g, 0.0115 mol) with acetic acid (16 mL) and 30% H_2O_2 (4 mL) and placed on a hot plate at 70 °C for 4 h. 30% H_2O_2 (4 mL) was added and left on the hot plate at 70 °C for another 4 h. A brown solid (0.2898 g, 14%) was collected via vacuum filtration: mp = 249-253 °C (lit mp = 256-257 °C)[41]; R_f = 0.16 (50:50 Hexanes:EtOAc); ^{1}H and ^{13}C NMR were not determined in time for this report.

REFERENCES

(1) Raff, Martin. Cell suicide for beginners. *Nature* 396(**1998**): 119-122.

(2) Thornberry, N. A., Lazebnik, Y. "Caspases: Enemies Within" *Science* **1998**, *281*, 1312-1316.

(3) Adrain, C., Creagh, E. M., and Martin, S. J. Caspase Cascades in Apoptosis. Caspases-their role in cell death and cell survival. Ed. Marek Los and Henning Walczak. Molecular Biology Intelligence Unit 24. New York: New York, 2002. 41-51.

(4) Isabel, E.; Black, W. C.; Bayly, C.I.; Grimm, E. L.; Janes, M. K.; McKay, D. J.; Nicholson, D. W.; Rasper, D. M.; Renaud, J.; Roy, S.; Tam, J.; Thornberry, N. A.; Vaillancourt, J. P.; Xanthoudakis, S.; Zamboni, R. "Nicotinyl Aspartyl Ketones as Inhibitors of Casapase-3" *Bioorg. Med. Chem. Lett.* **2003**, *13*, 2137-2140

(5) Caserta, T.M.; Smith, A.N.; Gultice, A.D.; Reedy, M.A.; Brown, T.L. "Q-VD-OPH, a broad spectrum caspase inhibitor with potent antiapoptotic properties" *Apoptosis* **2003**, *8*, 345-352.

(6) Renolleau, S.; Fau, S.; Goyenvalle, C.; Joly, L.M.; Chauvier, D.; Jacotot, E.; Mariani, J.; Charriaut-Marlangue, C. "Specific caspase inhibitor Q-VD-OPh prevents neonatal stroke in P7 rat: a role for gender" *J. Neurochem.*, **2007**, *100*, 1062-1071.

(7) Yang, L.; Sugama, S.; Mischak, R. P.; Kiaei, M; Bizat, N.; Brouillet, E.; Joh. T. H.; Beal, M. F. "A novel systemically active caspase inhibitor attenuates the toxicities of MPTP, malonate, and 3NP in vivo" *Neurobiol. Disease* **2004**, *17*, 250-259.

(8) Lee, D.; Long, S.A.; Murray, J.H.; Adams, J.L.; Nuttall, M.E.; Nadeau, D.P.; Kikly, K.; Winkler, J.D.; Sung, C.-M.; Ryan, M.D.; Levy, M.A.; Keller, P.M.; DeWolf, W.E. Jr. "Potent and selective nonpeptide inhibitors of caspases 3 and 7" *J. Med. Chem*. **2001**, *44*, 2015-2026.

(9) Chu, W.; Zhang, J.; Zeng, C.; Rothfuss, J.; Tu, Z.; Reichert, D.E.; Welch, M.J.; Mach, R.H. "N-Benzylisatin sulfonamide analogues as potent caspase-3 inhibitors: synthesis, in vitro activity, and molecular modeling studies" *J. Med. Chem*. **2005**, *48*, 7637-7647.

(10) Chu, W.; Rothfuss, J.; Chu, Y.; Zhou, D.; Mach, R. H. "Synthesis and in Vitro Evaluation of Sulfonamide Isatin Michael Acceptors as Small Molecule Inhibitors of Caspase-6" *J. Med. Chem*. **2009**, *52*, 2188-2191.

(11) Mofford, D.M.; Brush, E.J. "Design, synthesis and evaluation of indole and oxindole aspartic acid derivatives as potential caspase inhibitors." 231st ACS National Meeting, Atlanta, GA, March 26-30, **2006**.

(12) Löser, R.; Abbenante, G.; Madala, P.; Halili, M.; Le, G. T.; Fairlie, D. "Noncovalent Tripeptidyl Benzyl- and Cyclohexyl-Amine Inhibitors of the Cysteine Protease Caspase-1" *J. Med. Chem*. **2010**, *53*, 2651-2655.

(13) Sumpter, W.C.; Miller, M.; Magan, M.E. “The structure of Baeyer’s nitro-oxindole” *J. Am. Chem. Soc.* **1945**, *67*, 499-500.

(14) Vine, Kara L.; Locke, Julie M.; Ranson, Marie; Pyne, Stephen G.; Bremner, John B. “In vitro cytotoxicity evaluation of some substituted isatin derivatives” *Bioorg. Med. Chem*. **2007**, *15*, 931-938.

(15) Bruice, P. Y.; ‘Organic Chemistry” Pearson Education, Delhi, India; 3rd Edition: **2002**, 613-622.

(16) Sun, L.; Tran, N.; Liang, C.; Tang, F.; Rice, A.; Schreck, R.; Waltz, K.; Shawver, L.K.; McMahon, G.; Tang, C. “Design, synthesis, and evaluations of substituted 3-[(3- or 4-carboxyethylpyrrol-2-yl)methylidene]indolin-2-ones as inhibitors of VEGF, FGF, and PDGF receptor tyrosine kinases” *J. Med. Chem.* **1999**, *42*, 5120-5130.

(17) Somasekhara, S.; Dighe, V.S.; Suthar, G.K.; Mukherjee, S.L. “Chlorosulphonatiion of isatin” *Curr. Sci.* **1965**, 508.

(18) Abramovich, R. A.; Hey, D. H., *J. Chem. Soc.* **1954**, 1697

(19) Olgen, S.; Gotz, C.; Jose, J. “Synthesis and Biological Evaluation of 3-(substituted-benzylidende)-1,3-dihydro-indolin Derivatives as Human Protein Kinase CK2 and $p60^{c\text{-}Src}$ Tyrosine Kinase Inhibitors” *Biol. Pharm. Bull.* **2007**, *30*, 715-718.

(20) Crestini, C.; Saladino, R. “A new efficient and mild synthesis of 20oxindoles by one-pot Wolff-Kishner reduction of Isatin derivatives.” *Synth. Commun.* **1994**, *24*, 2835-2841.

(21) Bruice, P. Y.; 'Organic Chemistry" Pearson Education, Delhi, India; 3rd Edition: **2002**, 843-847.

(22) Sun, L.; Tran, N.; Tang, F.; App, H.; Hirth, P.; McMahon, G.; Tang, C. "Synthesis and biological evaluations of 3-substituted indolin-2-ones: a novel class of tyrosine kinase inhibitors that exhibit selectivity toward particular receptor tyrosine kinases" *J. Med. Chem*. **1998**, *41*, 2588-2603.

(23) Lotter, A.N.C.; Pathak, R.; Sello, T.S.; Fernandes, M.A.; van Otterlo, W.A.L.; de Koning, C.B. "Synthesis of the dibenzopyrrocoline alkaloid skeleton: indolo-[2,1-a]isoquinolines and related analogues" *Tetrahedron* **2007**, *63*, 2263-2274.

(24) Ivachtchenko, A.V.; Il'yin, A.P.; Kobak, V.V.; Zolotarev, D.A.; Boksha, L.V.; Trifilenkov, A.S.; Uglova, D.M. "New scaffolds for combinatorial synthesis. 1. 5-Sulfamoylisatins and their reactions with 1,2-diamines" *J. Comb. Chem*. **2002**, *4*, 419-428.

(25) Sumpter, W. C.; Jones, W. F. "The nitration of isatin." *J. Am. Chem. Soc*. **1943**, *65*, 1802-1803.

(26) Zhang, W.; Mei-Lin, G. "Functionalized 3-benzylidene-indolin-2-ones: Inducers of NAD(P)H-quinone oxidoreductase 1 (NQ01) with antiproliferative activity." *Bioorg. Med. Chem.* **2007**, *17*, 2077-2090.

(27) Coda, A. C.; Invernizzi, A. G.; Righetti, P. P.; Tacconi, G. "(Z)- and (E)-Arylidene-1,3-dihydroindol-2-ones: Configuration, Conformation, and Infrared Carbonyl Stretching Frequencies." *J. Chem. Soc. Perkin Trans. II* **1984**, 615-619.

(28) Wahl, A.; Bagard, P. *Compt. Rend*. **1909**, *149*, 132-4.

(29) Herz, W.; Murty, D. R. K. “Pschorr cyclizations in the pyridine series. The synthesis of Benz[*f*]- and Benz[*h*]isoquinoline.” *J. Org. Chem.* **1961**, *26*, 418-422.

(30) Lathourakis, G. E.; Litinas, K. E. “Synthesis and study of 3-(triphenylphosphoranylidene)-2,3-dihydro-1*H*-indol-2-one.” *J. Chem. Soc. Perkin Trans.* **1996**, 490-493.

(31) Villemin, D.; Martin, B. “Potassium Fluoride on Alumina: Dry synthesis of 3-arylidende-1,3-dihydro-indol-2-one under microwave irradiation.” *Synth. Commun*. **1998**, *28*(17), 3201-3208.

(32) Balderamos, M.; Ankati, H.; Akubathini, S.; Patel, A; Kamila, S.; Mukherjee, C.; Wang, L.; Biehl, E.; D’Mello, S. “Synthesis and structure-activity relationship studies of 3-substituted Indolin-2-ones as effective neuroprotective agents.” *Exp. Biol. Med.* **2008**, *233*, 1395-1402.

(33) Gassman, P. G.; Gilbert, D. P.; Luh, T. “Substituent effects on the Carbon-13 spectra of oxindoles.” *J. Org. Chem.* **1977,** *42*, 1340-1344.

(34) Kapiller-Dezsofi, R.; Volk, B.; “Interpretation of substituent-induced ^{13}C NMR chemical shifts of oxindoles.” *New J. Chem*. **2004**, *28*, 1218-1220.

(35) Conus, S.; Simon, H. “Cathepsins: Key modulators of cell death and inflammatory responses.” *Biochem. Pharm.* **2008**, *76*, 1374-1382.

(36) Camins, A.; Crespo-Biel, N.; Junyent, F.; Verdauger, E.; Cannudas, A.; Pallas, M. “Calpains as a target for therapy of neurodegenerative diseases: Putative role of Lithium.” *Curr. Drug Metabolism* **2009**, *10*, 433-447.

(37) Brnjic S.; Olofsson, M.H.; Havelka, A. M.; Linder, S. “Chemical biology suggests a role for calcium signaling in mediating sustained JNK activation during apoptosis.” *Mol. Biosyst.* **2010**, *6*(5), 767-74.

(38) Ho, W.; et al. “Synthesis and Anti-HIV-1 activity of 4,5,6,7-tetrahydro-4-methylimidazo-[4,5,1-*jk*][1,4]benzodiazepine-2(1H)-one (TIBO) Derivatives.” *J. Med. Chem*. **1995**, *38*, 794-802.

(39) Nakashima, T.; Suzuki, I. “Ring contraction of 3-hydroxyquinolines to oxindoles with hydrogen peroxide in acetic acid.” *Chem. Pharm. Bull*. **1969**, *11*, 2293-2298.

(40) Suzuki, I.; Nakashima, T.; Nagasawa, N. “Studies on Cinnolines: Oxidation of 5- and 8-nitrocinnoline.” *Chem. Pharm. Bull*. **1965**, *6*, 713-716.

(41) Coutts, R. T.; Hindmarsh, K. W.; Mah, E. “Preparation and properties of 5-nitro-, 7-nitro-, and 5,7-dinitrooxindole.” *Can. J. Chem*. **1970**, *48*, 3747-3749.

(42) Van Der Plas, H. C.; Buurman, D. J. “Ring transformation of heterocycles by oxidizing agents. A ^{14}C study of the conversion of quinolines into indoles by hydrogen peroxide.” *Chem. Pharm. Bull*. **1975**, *23*, 2682-2685.